Developmental Biology 339 (2010) 477–492

Contents lists available at ScienceDirect

Developmental Biology

journal homepage: www.elsevier.com/developmentalbiology

Delta-Notch signaling is involved in the segregation of the three germ layers in *Xenopus laevis*

Diego R. Revinski, Alejandra R. Paganelli, Andrés E. Carrasco, Silvia L. López *

Laboratorio de Embriología Molecular, Instituto de Biología Celular y Neurociencias, Facultad de Medicina, Universidad de Buenos Aires, Paraguay 2155, 3° piso (1121), Ciudad Autónoma de Buenos Aires, Argentina

ARTICLE INFO

Article history:
Received for publication 8 September 2009
Revised 6 January 2010
Accepted 7 January 2010
Available online 15 January 2010

Keywords:
Notch
Delta
Endoderm
Mesoderm
Neural ectoderm
Germ layers
Gastrulation
Xenopus laevis

ABSTRACT

In vertebrates, the induction of the three germ layers (ectoderm, mesoderm and endoderm) has been extensively studied, but less is known about how they segregate. Here, we investigated whether Delta-Notch signaling is involved in this process. Activating the pathway in the marginal zone with Notch^{ICD} resulted in an expansion of endodermal and neural ectoderm precursors, leaving a thinner mesodermal ring around the blastopore at gastrula stage, when germ layers are segregated. On the other hand, when the pathway was blocked with Delta-1^{STU} or with an antisense morpholino oligonucleotide against Notch, the pan-mesodermal *brachyury (bra)* domain was expanded and the neural border was moved animalwards. Strikingly, the suprablastoporal endoderm was either expanded when Delta-1 signaling was blocked, or reduced after the general knock-down of Notch. In addition, either activating or blocking the pathway delays the blastopore closure. We conclude that the process of delimiting the three germ layers requires Notch signaling, which may be finely regulated by ligands and/or involve non-canonical components of the pathway. Moreover, Notch activity must be modulated at appropriate levels during this process in order to keep normal morphogenetic movements during gastrulation.

Introduction

During vertebrate development, the process of gastrulation results in the formation of the three germ layers: ectoderm, mesoderm and endoderm. While their induction has been thoroughly studied (Yasuo and Lemaire, 2001; Stern, 2005), less is known about the mechanisms underlying their segregation. An early fate map of *Xenopus laevis* embryos has allowed tracing back the origin of the germ layers to the 32-cell stage (Dale and Slack, 1987). Their spatial domains are roughly depicted along the animal–vegetal axis: while the animal blastomeres (A-tier) and the vegetal blastomeres (D-tier) mostly contribute to ectoderm and endoderm, respectively, the mesoderm arises from both equatorial tiers (B and C). Interestingly, B-tier descendants were also found in ectodermal derivatives in a significant proportion, while the C tier also contributes to endoderm. For example, 48% of the brain derived from the progeny of blastomeres A1 and A2, while 40% derived from B1 and B2; 47% of the spinal cord derived from blastomeres B1 to B3, 32% derived from C2 and C3 while only 15% derived from A1 and A2; 53% of the notochord derived from C1 and C2, while 41% derived from B1; 64% of the somites derived from blastomeres C2 to C4, while 31% derived from the whole B tier; 82% of the endoderm derived from the whole D tier, while the remaining 18% derived from the whole C tier (see Fig. 3 from Dale and Slack, 1987). Therefore, although it is accepted that the mesoderm mainly develops from the equatorial region of the blastula, the fates of the equatorial tears are significantly mixed in terms of germ layers. Since a fate map of high resolution is not available at later stages in *Xenopus*, it is not known how the three germ layers segregate.

In Deuterostomes, germ layer specification is correlated with the complementary expression of Sox transcription factors of the B1- and the F-type along the animal-vegetal axis. In *X. laevis* embryos, the animal region expresses B1-type Soxs, such as Sox3, which suppresses mesendodermal and favors ectodermal development. On the other hand, the vegetally localized F-type Sox7 promotes mesendodermal development. Both appear to specify the germ layers by repressing or activating Nodal signaling in the animal and vegetal hemispheres, respectively. At the same time, Sox3 induces genes whose products are involved in ectodermal development (*ectodermin, Xema*), and Sox7 induces genes that participate in mesodermal (*slug, snail*) or endodermal development (*sox17, endodermin*) (Zhang and Klymkowsky, 2007).

All Metazoans studied so far express components of the Notch signaling pathway. One of its paradigmatic roles is sometimes referred to as 'inhibitory Notch signaling', which prevents equipotent cells from all adopting the same fate (Lai, 2004). This is classically illustrated by the lateral inhibition process during neurogenesis. Within a proneural cluster, more cells than necessary are competent to become neurons. However, the future neuron is the source of the

* Corresponding author. Fax: +5411 5950 9626.
E-mail address: slopez@fmed.uba.ar (S.L. López).

0012-1606/$ – see front matter © 2010 Elsevier Inc. All rights reserved.
doi:10.1016/j.ydbio.2010.01.010

membrane-bound ligand Delta, which interacts with the receptor Notch on the surface of the neighboring cells. This triggers two successive proteolytic cleavages, the second one in charge of the γ-secretase enzymatic complex, which cleaves the receptor within the transmembrane domain, releasing its intracellular domain ($Notch^{ICD}$). In the absence of Notch signaling, a member of the CSL family of proteins forms part of a repressor complex that inhibits the transcription of Notch-target genes. When the pathway is activated by the ligand, $Notch^{ICD}$ enters the nucleus, the co-repressors are displaced, and co-activators are recruited. This newly formed complex, containing $Notch^{ICD}$ and CSL, activates the transcription of target genes that lead to the suppression of the neuronal fate in the cells surrounding the neuronal precursor (Lai, 2004; Fortini, 2009).

This cascade of events describes the canonical Notch signaling pathway, which is the best studied until now. However, there is growing evidence that Notch sometimes functions through non-canonical mechanisms which do not involve CSL transcription factors. Moreover, other ligands distinct from the Delta-Serrate family may participate, and even Notch-dependent, non-nuclear mechanisms that may involve cytoskeleton interactions were proposed for axon guidance (Hu et al., 2003; Hori et al., 2004; Langdon et al., 2006; Mizutani et al., 2007; D'Souza et al., 2008; Le Gall et al., 2008).

In addition to the 'inhibitory Notch signaling', Notch is often involved in cell–cell interactions at the boundary between non-equivalent cell populations, where it is able to induce a distinct cell type by controlling the expression of positively acting regulatory molecules. This role is sometimes referred to as 'inductive Notch signaling'. The best known example is the development of the future wing in flies, where Notch is responsible for creating the dorsal–ventral boundary (Lai, 2004; Fortini, 2009). Other examples include early blastomere determinations in *C. elegans* and tip-cell formation during mammalian angiogenesis (Good et al., 2004; Benedito et al., 2009).

Components of the Notch pathway are present in *Xenopus* from early stages of embryogenesis. Maternal and zygotic expression has been reported for transcripts encoding the receptor Notch, the ligand Serrate-1 and the CSL transducer Su(H)1 (Coffman et al., 1990; Kiyota et al., 2001; Ito et al., 2007). Interestingly, although it was not addressed whether the mRNAs for the ligands Delta-1 and Delta-2 are present maternally, their expression becomes detectable by in situ hybridization (ISH) at early gastrula in the marginal zone, in a ring encircling the blastopore, where Notch transcripts are enriched and epithelial–mesenchymal transitions and involution of the mesoderm are taking place (Ma et al., 1996; López et al., 2003; Shook and Keller, 2003; Abe et al., 2004). Moreover, *delta-1* transcripts are present in the pre-involuted mesoderm but disappear from the involuted cells (Wittenberger et al., 1999). In addition, there is some evidence that Notch signaling is active in the animal hemisphere before the beginning of gastrulation in *Xenopus* (Mir et al., 2008).

It has been previously described a role for Notch signaling in the development of the dorsal midline derivatives in Vertebrates. In *Xenopus* embryos, Notch favors the development of the floor plate at the expense of the notochord (López et al., 2003, 2005). In zebrafish, Notch expands the floor plate population and favors hypochord development at the expense of the notochord (Latimer and Appel, 2006). Loss-of-function of *delta-1* results in an excess of floor plate cells in mouse, while the notochord is reduced (Przemeck et al., 2003). The opposite activities of Delta-Notch signaling in mouse and anamniotes embryos are intriguing; nevertheless, they underscore a role for this pathway in the development of the dorsal midline structures. In addition, although neural or paraxial mesoderm markers were not assayed, we observed that transverse sections of *Xenopus* neurulae injected with $notch^{ICD}$ mRNA showed a thicker neural plate and a thinner paraxial mesoderm (Fig. 2A in López et al., 2003). Therefore, we wondered if the Delta-Notch function described for the dorsal midline derivatives is extended over neural and mesodermal development.

Several authors, by using *Xenopus* embryos and different constructions encoding constitutively active forms of Notch, described a variety of changes in muscle and neural differentiation markers at tailbud stages. The main contradiction between those works is the outcome on mesodermal development. For instance, Coffman et al. (1993), which employed *notch ΔE* (a constitutively active construction lacking the extracellular domain of Notch but conserving the transmembrane domain) found an increase of both types of markers (N-CAM, for neural differentiation, and 12/101 for muscle differentiation), and the extra tissue arose even if proliferation was blocked at late gastrulation. Kopan et al. (1994) injected a constitutively active $notch^{ICD}$ mRNA of mouse origin and observed a decrease of the muscle differentiation marker myosin, instead. On the other hand, the activation of the pathway before gastrulation by means of a hormone-inducible construct of $notch^{ICD}$ increased the muscle differentiation marker 12/101 in tailbuds and the expression of the neural marker *sox2* in neurulae. However, these changes did not occur if the pathway was activated at the end of gastrulation (Glavic et al., 2004). Contakos et al. also employed hormone-inducible constructs and examined their results from late neurula onwards. Activation of $Notch^{ICD}$- or CSL-dependent signaling at stage 10 produced an expansion of endodermal markers and a reduction of mesodermal markers, while blocking CSL signaling at the same stage gave the opposite results. Strikingly, when hormone was added at stage 14, the tendency was reversed for some markers: activation of CSL-dependent signaling led to an increase of two pronephric markers and to a reduction of *endodermin*, while inhibition led to the opposite changes (Contakos et al., 2005). However, neither of these works analyzed early markers of mesoderm specification. They were mostly focused on advanced stages of development, long after the segregation of germ layers. This could complicate the interpretation of results due to the superposition of different effects of Notch through time in a variety of process (i.e.: differentiation, somitogenesis). In addition, the possibility that Notch could be selecting between neural ectoderm and mesoderm as alternative fates was not addressed.

In this work we study whether Delta-Notch signaling is involved in the segregation of the three germ layers. To address this issue, we studied the expression of neural, endodermal and mesodermal markers at gastrula and early neurula stages in embryos where Notch signaling was manipulated. The pathway was activated by injection of $notch^{ICD}$ mRNA and blocked by injection of $su(H)1^{DBM}$ mRNA, $delta\text{-}1^{STU}$ mRNA, an antisense morpholino oligonucleotide against Notch (López et al., 2003) or by treatments with DAPT, an inhibitor of γ-secretase (Latimer and Appel, 2006). We show that Notch signaling is involved in delimiting the three germ layers during gastrulation and this may be finely regulated by Notch ligands and/or non-canonical components of the pathway. Moreover, Notch activity must be modulated at appropriate levels in order to keep normal morphogenetic movements during gastrulation.

Materials and methods

Embryological manipulations, RNA synthesis, morpholinos and injections

Albino and wild type *X. laevis* embryos were obtained using standard methods and staged according to Nieuwkoop and Faber (1994).

Synthetic capped mRNAs for microinjection were obtained as described (Franco et al., 1999). The injections were delivered into the animal hemisphere of one blastomere at the 2 or 4-cell stage at approximately 30–40° from the equator. The templates for $notch^{ICD}$, $su(H)1^{DBM}$ and $delta\text{-}1^{STU}$ mRNA synthesis were described before (Chitnis et al., 1995; Wettstein et al., 1997). The Notch morpholino antisense oligonucleotide (Notch Mo) and the standard control morpholino (Control Mo) were modified with 3′-fluorescein and

were used as previously described (López et al., 2003). The injected amounts of synthetic mRNAs and morpholinos are indicated in the figures and tables. Some injections included molecular tracers such as mRNA of Green Fluorescent Protein (GFP; 2 ng were injected in sibling controls and 1 ng in co-injections), 10 ng of Dextran Oregon Green (DOG, Molecular Probes) or 20 ng of Biotin Dextran Amine (BDA, Molecular Probes). The co-injections are indicated in the figures.

To measure the blastopore size, pigmented embryos of the same batch and obtained from eggs of the same female were injected before the first mitotic division with 1 ng of *notch*^{ICD} mRNA + 1 ng of *GFP* mRNA as tracer, 2 ng of *GFP* mRNA (as negative control of the *notch*^{ICD} mRNA injections), 20 ng of Notch Mo or 20 ng of Control Mo. At the beginning of gastrulation, injected embryos were selected by fluorescence and placed on a clear plastic dish. The vegetal hemispheres were photographed with a digital scanner at high resolution at different times during gastrulation, as previously described (Ueno et al., 2006). Measurements were made with Image Pro. Since *notch*^{ICD} greatly impaired the formation and progress of the blastopore, its limits at early gastrula were poorly defined except from the dorsal side. Thus, we chose to measure the perimeter of the slit instead of the diameter of the blastopore. The ratio between the perimeter of the blastopores and the perimeter of embryos was calculated as the indicator in the progression of gastrulation.

In situ hybridization, immunodetections and histology

The preparation of digoxigenin-labeled antisense RNA probes and whole-mount in situ hybridization (ISH) were performed as described previously (Pizard et al., 2004), except that the proteinase K step was omitted. For double ISH, fluorescein-labeled antisense RNA probes were prepared with fluorescein-12-UTP (Roche) and embryos were revealed in the first step with BCIP, and on the second step with NBT + BCIP as previously described (López et al., 2005). To avoid cross-reactions with fluoresceinated morpholinos or with DOG in the detection steps, in some double ISH we used a *chordin (chd)* probe labeled with biotin-16-UTP and an anti-biotin-AP conjugated monoclonal antibody (Roche) diluted 1/3000 in 2% Blocking Reagent.

To reveal the BDA tracer, embryos were washed twice for 10 min each with binding buffer (100 mM Tris–HCl, pH 7.5; 150 mM NaCl) and incubated overnight at room temperature with alkaline phosphatase-conjugated Streptavidin (Streptavidin-AP, Roche) diluted 1/5000 in binding buffer. Then, embryos were washed two times for 10 min each with binding buffer. Streptavidin-AP was revealed with BCIP or Magenta Phos as substrates (Biosynth) as in double ISH.

In some experiments, the injected side was identified before the ISH procedure by the fluorescence of DOG, GFP or the morpholinos, but with large number of samples, the time consuming step of classification before dehydrating impaired the quality of the ISH results. Because the fluorescence of the tracers decreased after the ISH procedure, we revealed GFP and DOG by immunofluorescence.

The c-myc epitope contained in the *notch*^{ICD} or *su(H)1*^{DBM} constructs used for mRNAs injections was revealed by immunodetection. In some embryos, the c-myc epitope or the 3′-fluorescein morpholinos were revealed by HRP or alkaline phosphatase immunostainting, respectively, as described (López et al., 2005). Because the colored immunoprecipitate sometimes obscured the ISH results in whole embryos, in several experiments the c-myc epitope and the morpholinos were revealed by inmunofluorescence. For this, embryos were first incubated with anti-Myc, as indicated previously, following by 4 h incubation at room temperature with anti-mouse IgG-FITC (DAKO) diluted 1/200 in 2% Blocking Reagent. The unbound antibodies were washed three times, 5 min each, with MAB.

For GFP detection, embryos were incubated with mouse B-2 anti-GFP monoclonal antibody (Santa Cruz) diluted 1/100 in 2% Blocking Reagent and the excess of antibody was removed as above. Then, they were incubated with anti-mouse IgG-FITC (DAKO) as before. For DOG detections, embryos were incubated with goat IgG anti-Fluorescein/Oregon Green-Alexa Fluor 488-conjugated antibody (Molecular Probes) diluted 1/100 in 2% Blocking Reagent. The excess of antibody was removed as above. This antibody also recognizes the 3′-fluorescein modified morpholinos, but the immunofluorescence quality improved when DOG was co-injected with them.

For histology, 50 μm sections were taken in an Oxford Vibratome and 20 μm sections were taken in a microtome. They were mounted onto gelatine coated slides.

DAPT treatments

The γ-secretase inhibitor *N*-[*N*-(3,5-Difluorophenacetyl-L-alanyl)]-*S*-phenylglycine-*t*-Butyl Ester (DAPT, Calbiochem) was reconstituted with DMSO to make a stock concentration of 10 mM (Latimer and Appel, 2006). Embryos were incubated with 100 μM DAPT in 0.1× Modified Barth's Saline (MBS) from stage 1 to stage 11 or 14. Sibling controls were incubated in vehicle alone in 0.1× MBS.

Results

Active Notch produces complementary changes on neural ectoderm and paraxial mesoderm at the neural plate stage

We activated Notch signaling by injecting 1 ng of *notch*^{ICD} mRNA into one cell of 2- or 4-cell stage embryos. Neural and paraxial mesoderm development was evaluated at neural plate stage by examining the effects on the expression of *sox2* (neural ectoderm) and the myogenic-related factors *myoD* and *myf5*. At this stage, *myoD* is expressed along the anterior–posterior extent of the presomitic mesoderm, while *myf5* transcripts are distributed mainly in the posterior region (Frank and Harland, 1991; Hopwood et al., 1991).

Notch^{ICD}-injected embryos showed different grades of impairment in the elongation and in the closure of the blastopore in relation to sibling controls (compare Figs. 1B, C with A). The *sox2* expression domain was considerably wider on the injected side (Figs. 1F, J; Table 1) and this was accompanied by an increase in the intensity of *sox2* staining (Fig. 1J). By contrast, the expression of *myoD* and *myf5* decreased on the injected side (Figs. 1B, C, F; Table 1). This was more clearly appreciated on transverse sections, which revealed that not only the neural plate is widened in the medio-lateral axis, but it is also thicker on the injected side (compare white bars in Figs. 1E, H, I and the thickness of the *sox2* domain between the injected- and the non-injected sides in Figs. 1F′, G, K). Remarkably, this change is complementary to a thinner paraxial mesoderm (Figs. 1E, F′, G–I). In some sections, the *myoD* staining is barely detectable on the injected side, while the neural ectoderm is extremely thickened and expresses very high levels of the recombinant Notch^{ICD} protein, as revealed by Myc-tag immunostaining (Fig. 1I). Interestingly, in sibling control embryos or in the non-injected side, two layers of paraxial mesoderm expressing *myoD* and *myf5* transcripts become discernible at this stage. The dorsal one is more constrained on the medio-lateral axis (compare green and yellow arrowheads in Figs. 1D, F′) and expresses higher levels of *myoD* or *myf5* transcripts than the ventral one (Figs. 1D, E, F′, G, H, green and yellow arrows). Notably, *notch*^{ICD}-injected embryos appear to preferentially loose the dorsal layer of the paraxial mesoderm, which seems to be replaced by the thicker neural ectoderm. The ventral layer of the paraxial mesoderm seems to be more refractory, despite expressing the Notch^{ICD} recombinant protein (Figs. 1E, F′, G, H). These results suggest that Notch may be favoring neural development at the expense of paraxial mesoderm. However, not all the mesodermal cells appear to respond uniformly to Notch activation, and this seems to be correlated with their dorsal/ventral allocation within the paraxial mesoderm.

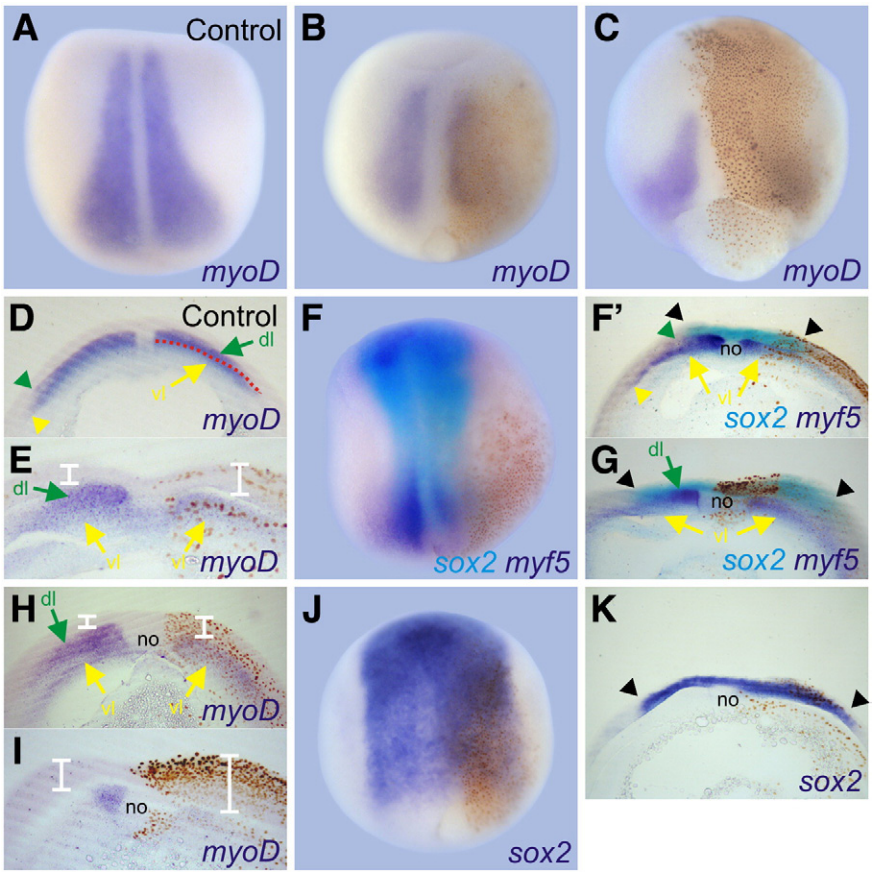

Fig. 1. Effects of Notch^{ICD} on neural and paraxial mesodermal markers at the neural plate stage. Embryos were injected with 1 ng of *notch^{ICD}* mRNA in one cell at the 2- or 4-cell stage and fixed at neural plate stage (B,C,E–K), when sibling control embryos reached stages 13–14 (A,D). They were revealed by ISH with the following probes: *myoD* (purple staining in A–E,H,I), *myf5* (purple staining in F–G) and *sox2* (turquoise staining in F–G; purple staining in J,K). Brown dots correspond to immunolocalization of the Myc-tag epitope fused to Notch^{ICD}. All photographs were oriented with the injected side towards the right. (D) Transverse section of the sibling control embryo shown in (A). Two layers are apparent in the paraxial mesoderm: one dorsal, expressing higher levels of *myoD* transcripts (dl, green arrow) and the other ventral, expressing lower levels of *myoD* transcripts (vl, yellow arrow). The dotted red line depicts the boundary between both layers and arrowheads point to their lateral limits (green: dl; yellow: vl). (E) Transverse section of an embryo injected with *notch^{ICD}* mRNA. The dorsal layer of paraxial mesoderm appears to be missing from the injected side (right), while the ventral layer remains. (F′) Transverse section of the embryo shown in F. (G) Transverse section of an embryo similar to the one shown in (F). The same references as in (D) are used for the dorsal and ventral layers of the paraxial mesoderm as revealed by *myf5* expression. (H) Transverse section of the embryo shown in (B). (I) Transverse section of the embryo shown in (C). White bars in (E,H,I) indicate the thickness of the neural ectoderm. no, notochord. Black arrowheads in (F′,G,K) point to the lateral limits of the *sox2* domain.

Notch activation alters the expression of markers of the three germ layers and impairs morphogenetic movements during gastrulation

It has been described that the activation of Notch signaling at early gastrula produces an expansion of the expression domain of many endodermal markers and a reduction of mesodermal markers (Contakos et al., 2005). However, these authors analyzed the phenotypes at late neurula, tailbud and tadpole stages, which could be the result of a sum of effects of active Notch at different times of development. To address whether Notch signaling can affect the three germ layers at the time of their segregation, we activated the pathway and evaluated the consequences at the gastrula stage by comparing the effects on the expression of the pan-mesodermal marker *bra*, the F-type transcription factor *sox17α* (endoderm) and the B1-type transcription factor *sox2* (neural ectoderm). At gastrula stages, *sox17a* is expressed in the blastoporal and suprablastoporal prospective endoderm (Hudson et al., 1997).

When observed in whole mount preparations, embryos injected with 1 ng of *notch^{ICD}* mRNA showed changes in the shape of the blastopore on the injected side (dotted red line, Figs. 2G, I). The intensity of the *bra* staining was decreased (Table 2; compare Fig. 2B with A, and E with D), while the area of the suprablastoporal *sox17α+* ring was increased as well as the *sox17α* staining in the blastoporal prospective endoderm (Table 2, Figs. 2G–H′) and the *sox2* staining around the marginal zone (Table 2, Fig. 2I). In overall, we observed an alteration in the width of the *bra* domain in 80% of the injected embryos ($n=64$), but the nature of the change depended on the distribution of the recombinant Notch^{ICD} protein. In a considerable proportion of embryos (28%) the *bra* domain was clearly thinner on the injected side. This was correlated with a strong Myc-tag immunofluorescence on the marginal zone (Figs. 2A–C). Another situation was observed when the recombinant Notch^{ICD} protein mostly located to the animal hemisphere, with lower levels on the marginal zone. These embryos show an expansion of the *bra* domain, but the staining was always more diffuse than on the non-injected side (52%; Figs. 2D–F). To better understand this variability, we performed histological sections. The intensity of *bra* staining was lower on the injected side in all cases (Figs. 2C′, F′), even in those embryos where the *bra* domains were expanded, which showed an increase in the number of *bra+* cells (Fig. 2F′). On the other hand, the thinner *bra* domains revealed a clear decrease in the number of *bra+* cells both in the pre-involuted and in the involuted mesoderm (Fig. 2C′). This is complementary to the up-regulation of *sox17α* and to the increase in the density of *sox17α+* cells in the suprablastoporal endoderm (arrow, Fig. 2H′). Moreover, the animal limit of *bra* staining in the pre-involuted mesoderm was displaced vegetalwards on the injected side (Fig. 2C′, compare arrowheads), and this is complementary to the increase of *sox2* expression in the marginal zone (Fig. 2I). These

Table 1
Effects of manipulating Notch signaling, evaluated at late gastrula and neural plate stage.

	myf5	myoD	sox2
notch^{ICD} 1 ng	↑5%, ↓90%, w/ch 5%; $n=19$ *Transverse sections:* Thickness: ↓6/6 (dorsal loss complementary to ↑thickness of *sox2*; double ISH).	↑8%, ↓67%, w/ch 25%; $n=12$ *Transverse sections:* Thickness: ↓5/7 (dorsal loss complementary to ↑thickness in neural ectoderm) Intensity: ↓2/7	↑94%, ↓3%, w/ch 3%; $n=31$ *Transverse sections:* Thickness: ↑15/15 ML: ↑14/15, ↓1/15
su(H)1^{DBM} 2 ng	↑47%, ↓26%, w/ch 26%; $n=19$ *Transverse sections:* Thickness: ↑3/7 Intensity: ↑2/7 ML: ↑3/7	*Transverse sections:* Thickness: ↑1/10 Intensity: ↑5/10 ML: ↑2/10	ML: ↑20%, ↓52%, w/ch 28%; $n=25$ *Transverse sections:* Thickness: ↑2/16, ↓5/16 ML: ↑3/16, ↓10/16
delta-1^{STU} 0.5–1 ng	↑100% (area and intensity); $n=7$	↑100%; $n=8$	ML: ↑9%, ↓41%, w/ch 50%; $n=22$
Control Mo 20 ng	NA	*st 12–13:* ↑10%, ↓7%, w/ch 83% $n=29$ *st 14–15:* ML: ↑0%, ↓0%, w/ch 100% Intensity: ↑4%, ↓4%, w/ch 92% $n=23$	*st 12–12.5:* ML: ↑7%, ↓3%, w/ch 90% Intensity: ↑7%, ↓7%, w/ch 86% $n=29$ *st 12.5–13:* ML: ↑27%, ↓0%, w/ch 73% Intensity: ↑27%, ↓0%, w/ch 73% $n=11$ *st 14–15:* ML: ↑3%, ↓22%, w/ch 75% Intensity: ↑19%, ↓3%, w/ch 78% $n=32$
Notch Mo 20 ng	NA	*st 12–13:* ↑73%, ↓9%, w/ch 18% $n=44$ *st 14–15:* ML: ↑74%, ↓0%, w/ch 26% Intensity: ↑62%, ↓3%, w/ch 35% $n=34$	*st 12–12.5:* ML: ↑17%, ↓46%, w/ch 37% Intensity: ↑46%, ↓12%, w/ch 42% $n=24$ *st 12.5–13:* ML: ↑26%, ↓5%, w/ch 69% Intensity: ↑38%, ↓8%, w/ch 54% $n=39$ *st 14–15:* ML: ↑54%, ↓2%, w/ch 44% Intensity: ↑33%, ↓0%, w/ch 67% $n=39$

Changes in the medio-lateral breadth (ML) of the domain of *myoD*, *myf5* and *sox2* and/or in the intensity of the ISH staining (except where indicated separately), as revealed by ISH in whole embryos. They were fixed when sibling controls reached stages 13–14, except where indicated. ↑: increase; ↓: decrease; w/ch: without changes. NA: not analyzed. Results are given as the percentage of embryos displaying the indicated change. *n*: total number of embryos analyzed. Some specimens were evaluated on transverse sections, and results are given as the ratio between the number of embryos displaying the indicated changes and the total number of embryos analyzed by histology. Changes observed with Control Mo are qualitatively milder than those observed on the other experimental situations and may reflect normal asymmetries in the expression pattern. See text for additional details.

changes are compatible with a vegetal displacement of the limit of involution and with the increase of endoderm at the expense of mesoderm.

Active Notch also altered the expression of *myf5*, whose expression is first visible in two symmetrical dorsolateral domains in the early gastrula, marking precursors of the somitic mesoderm (Hopwood et al., 1991). When sibling controls reached stage 11, *notch*^{ICD}-injected embryos showed a decrease of *myf5* expression, which was often accompanied by changes in the shape of the domain (Table 2; Figs. 3A, D, G). Parasagittal sections confirmed that the effect on *myf5* varied from almost a complete disappearance of transcripts on the injected side (compare Figs. 3F with E) to down-regulations mainly confined to the animal and vegetal borders of the domain, which appears thinner in whole embryos (compare Fig. 3I with H). Changes in the shape of the domain, as illustrated by the embryo shown in Fig. 3A, were correlated with an increase of *myf5+* cells in the superficial layer and with a decrease in the deep layer of the mesoderm (compare Fig. 3C with B), suggesting that involution was impaired on the injected side.

To determine whether an excess of Notch activity alters the morphogenetic movements during gastrulation, we compared the size of the blastopore between *notch*^{ICD} mRNA- and *GFP* mRNA-injected embryos at different times. A very significant delay in the progress of the blastopore was observed in *notch*^{ICD}-injected embryos when compared to *GFP*-injected siblings (Table 3). This alteration persisted throughout gastrulation and was most remarkable during early and midgastrula stages. Eventually, the blastopore tended to close towards the end of gastrulation, but even at stage 12 it was slightly larger in *notch*^{ICD}-injected embryos. Figs. 3J–N illustrate a representative experiment.

Therefore, activation of Notch signaling results in an increase of the expression of endodermal and neural markers in the marginal zone during gastrulation, whereas the domain of the pan-mesodermal marker *bra* is expanded or reduced, which seems to depend on the distribution of the injected mRNA. Nevertheless, judging from the intensity of the staining, *bra* appears to be down-regulated in the marginal zone. These changes are accompanied by alterations in morphogenetic movements during gastrulation, as evidenced by changes in the blastopore shape, delays in the blastopore closure and impairment in the involution of *myf5+* cells.

Blocking of Delta-Notch signaling shifts the boundaries of the three germ layers at the gastrula stage and impairs morphogenetic movements during gastrulation

The overexpression experiments suggest that activation of Notch signaling can alter the expression of neuroectodermal, mesodermal and endodermal markers at the boundaries of the three germ layers when they segregate during gastrulation. Moreover, the expression pattern of the ligands (see Introduction) indicates that Delta-Notch signaling is preferentially active around the blastopore from stages 10.5 or 11. Therefore, ectopic activation of this pathway in other regions may lead to confusing results. For example, it has been reported that when activated in the animal cap, Notch can delay the loss of mesodermal competence of the ectoderm that normally takes

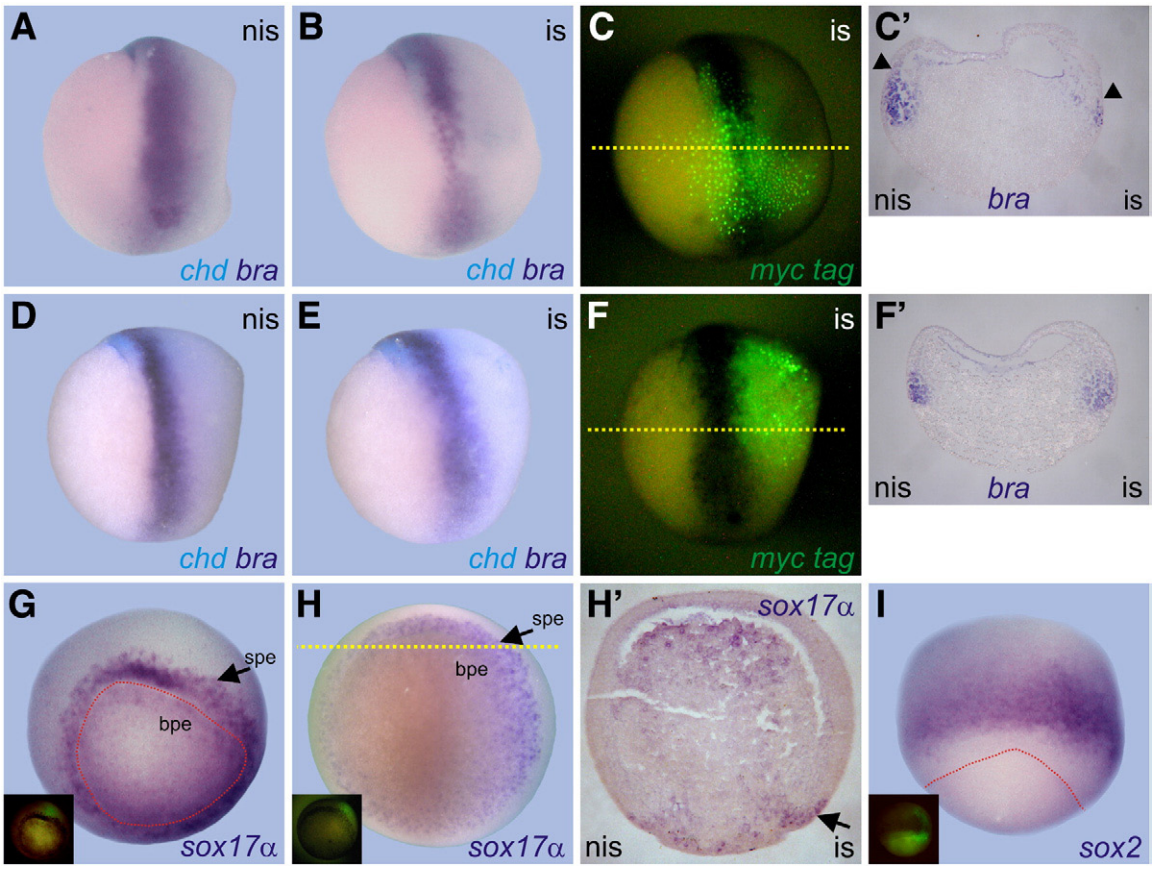

Fig. 2. Effects of Notch^{ICD} on markers of the three germ layers at gastrula stage. Embryos were injected with 1 ng of *notch^{ICD}* mRNA in one cell at the 4-cell stage and fixed when sibling control embryos reached stage 11. They were revealed by ISH with the following probes: *bra* (purple staining in A,B,C′,D,E,F′), *chd* (turquoise staining in A,B,D,E), *sox17α* (purple staining in G–H′) and *sox2* (purple staining in I). Green fluorescence corresponds to immunolocalization of the Myc-tag epitope fused to Notch^{ICD} (C,F and insets in G,H,I). (A–C,D–F) Lateral views of *notch^{ICD}*-injected embryos to show changes in the *bra* domain. The dorsal side (up) is marked by *chd* staining. Photographs were inverted to facilitate comparisons between the injected- and the non-injected sides. (G,H) Vegetal views of embryos injected with *notch^{ICD}* mRNA to show changes in *sox17α* expression. (I) Dorsal view of an embryo injected with *notch^{ICD}* mRNA to show changes in *sox2* expression. (C′,F′,H′) Sections in the planes shown by the yellow dotted lines in (C,F,H) respectively; animal is up, vegetal is down. Photographs in (C′,F′,G–I) were oriented with the injected side towards the right. nis: non-injected side; is: injected side; spe: subprablastoporal prospective endoderm; bpe: blastoporal prospective endoderm. Arrowheads in (C′) point to the animal border of the *bra* domain in the pre-involuted mesoderm. Arrows in (G–H′) point to the spe. The dotted red line in (G,I) demarcates the blastopore.

place during gastrulation (Coffman et al., 1993; Abe et al., 2004). This may explain the expansion of the *bra* domain in a considerable proportion of embryos in our experiments.

We reasoned that a loss-of-function strategy would clarify this situation, since it deals with the territories and cells where Delta-Notch signaling is actually taking place. Therefore, to understand whether this pathway is normally involved in the segregation of the three germ layers during gastrulation, we injected *su(H)1^{DBM}* mRNA to impair CSL-dependent, canonical Notch activity (Wettstein et al., 1997); *delta-1^{STU}* mRNA to block signaling by the ligand Delta-1 (Chitnis et al., 1995), or an antisense morpholino oligonucleotide against Notch (Notch Mo) to produce a general blockade of the Notch pathway (López et al., 2003).

Blocking CSL-dependent Notch signaling produced a mild expansion of the *bra* domain at the gastrula stage in a considerable proportion of embryos (Table 2; Supplementary Fig. 1A,A′) and a mild increase of *myf5* expression (Table 2). Although some specimens showed a reduction of *sox2* expression and a displacement of the vegetal border of the domain towards the animal pole (Supplementary Fig. 1B–B″), the results with *sox2* and *sox17α* were variable and did not show a clear tendency (Table 2). However, impairment of Delta-1 signaling or a general blockade of the Notch pathway consistently resulted in complementary shifts of the boundaries of the markers analyzed. Both strategies notably expanded the *bra* domain (Figs. 4A–B″, D–E) and shifted the *sox2* domain towards the animal pole, with a consistent down regulation of *sox2* at the marginal zone border (Figs. 4G–G″, I–J″). However, an important difference appeared between both approaches. While *delta-1^{STU}* expanded the suprablastoporal ring of *sox17α* (Fig. 4L), the Notch Mo decreased the number of *sox17α+* cells in this region (Fig. 7N). Interestingly, and compatible with the changes of *sox2* and *sox17α* expression, ISH of *bra* revealed that in *delta-1^{STU}*-injected embryos, the gap of unstained cells between the *bra+* ring and the blastopore was expanded (asterisk, Fig. 4B) while the *bra* domain was clearly shifted and expanded towards the animal region (arrows, Figs. 4A′, B″). On the other side, the Notch Mo expanded the *bra+* ring in both directions (compare bars in Figs. 4D′, E): vegetalwards (arrows in Fig. 4D′, green arrowhead in Fig. 4E) and animalwards (arrows in Fig. 4E). All these effects of Notch-Mo were reversed by *notch^{ICD}* mRNA, which does not contain the target sequence of the morpholino (Table 2; Figs. 4F, K, O). Injection of a Control Mo did not produce significant changes in either marker (Table 2; Figs. 4C, H–H″, M). Moreover, *notch^{ICD}* also reversed the Notch Mo phenotype on primary neurogenesis, as revealed by ISH of *N-tubulin* at the neural plate stage (Supplementary Fig. 2), supporting the specificity of the effects of Notch Mo.

To determine whether a general blockade of Notch activity alters the morphogenetic movements during gastrulation, we compared the size of the blastopore between Notch Mo- and Control Mo-injected embryos throughout the process. A significant delay in the closure of the blastopore was observed in Notch Mo-injected embryos when compared to Control Mo-injected siblings (Table 4). Although this

Table 2
Effects of manipulating Notch signaling, evaluated at early gastrula stage.

	bra	sox2	sox17α	myf5
notch^{ICD} 1 ng	width:↑52%, ↓28%, w/ch 20% intensity: ↑11%, ↓70%, w/ch 19% *n* = 64	↑64%, ↓16%, w/ch 20% *n* = 53	width:↑79%, ↓0%, w/ch 21% intensity: ↑38%, ↓19%, w/ch 43% *n* = 53	↑9%, ↓79%, w/ch 12% *n* = 42
su(H)1^{DBM} 2 ng	width:↑90%, ↓0%, w/ch 10% intensity:↑20%, ↓10%, w/ch 70% *n* = 10	↑34%, ↓46%, w/ch 20% *n* = 41	width:↑26%, ↓32%, w/ch 42% intensity:↑26%, ↓11%, w/ch 63% density:↑0%, ↓21%, w/ch 79% *n* = 19	↑47%, ↓26%, w/ch 26% *n* = 19
delta-1^{STU} 1 ng	width:↑78%, ↓3%, w/ch 19% intensity:↑29%, ↓32%, w/ch 39% *n* = 31	↑6%, ↓94%, w/ch 0% Distance from the blastopore: AW: 89%, VW: 0%, SD: 11% *n* = 18	width:↑85%, ↓0%, w/ch 15% intensity: ↑35%, ↓5%, w/ch 60% density:↑15%, ↓0%, w/ch 85% *n* = 20	↑72%, ↓27%, w/ch 0% *n* = 11
Control Mo 20 ng	↑22%, ↓4%, w/ch 74% *n* = 27	↑9%, ↓9%, w/ch 82% Distance from the blastopore: AW: 1%, VW: 1%, SD: 98% *n* = 65	↑13%, ↓7%, w/ch 80% *n* = 15	NA
Notch Mo 20 ng	↑88%, ↓6%, w/ch 6% *n* = 35	↑2%, ↓76%, w/ch 22% Distance from the blastopore: AW: 73%, VW: 0%, SD: 27% *n* = 55	↑16%, ↓74%, w/ch 10% *n* = 19	NA
Notch Mo 20 ng + notch^{ICD} 1 ng	↑21%, ↓79%, w/ch 0% *n* = 14	↑45%, ↓55%, w/ch 0% Distance from the blastopore: AW: 0%, VW: 45%, SD: 55% *n* = 20	↑65%, ↓12%, w/ch 23% *n* = 17	NA

Changes in the expression pattern of *bra*, *sox2*, *sox17α* and *myf5* after manipulating Delta-Notch activity, as revealed by ISH in whole embryos. They were fixed when sibling controls reached stage 11. ↑: increase; ↓: decrease; w/ch: without changes. Results are given as the percentage of embryos displaying the indicated change. *n*: total number of embryos analyzed. NA: not analyzed. *bra*: changes in the width of the domain, with or without changes in the intensity of the ISH staining, except where indicated separately. *sox2*: changes in the width of the domain and/or in the intensity of the ISH staining in the marginal zone. AW: the vegetal border of the *sox2* expressing domain is displaced animalwards. VW: the vegetal border of the *sox2* expressing domain is displaced vegetalwards. SD: the vegetal border of the *sox2* expressing domain on the injected-side is at the same distance from the blastopore than on the non-injected side. *sox17α*: changes in the width of the domain, and/or in the intensity of the ISH staining or in the density of *sox17α+* cells, except where indicated separately. *myf5*: changes in the width of the domain and/or in the intensity of ISH staining. Changes observed with Control Mo are qualitatively milder than those observed on the other experimental situations and may reflect normal asymmetries in the expression pattern.

alteration was observed at different times during gastrulation, the effect was milder in relation to *notch^{ICD}* mRNA injections, and the blastopore tends to close towards the end of the process. Fig. 5A illustrates a representative experiment.

Interestingly, embryos treated with the γ-secretase inhibitor DAPT from stage 1 to stage 11 and hybridized with the dorsal axial mesodermal marker *chd* showed that *chd+* cells were still accumulated in an arch on the dorsal blastopore lip (83%, *n* = 40). In contrast, sibling embryos treated with vehicle alone (DMSO) revealed that these cells have largely involuted and the domain has began to elongate (Figs. 5B, C). DAPT treatments from stage 1 to neurula stages consistently increased the number of *N-tubulin+* cells, as expected (85% of treated embryos, *n* = 53; Figs. 5D, E), demonstrating that DAPT is able to impair Notch signaling in vivo in *Xenopus*. These embryos also show that the blastopore is able to close and that *chd+* cells complete involution when gastrulation ends. Thus, after blocking the cleavage of Notch to render the active intracellular domain, the involution of the dorsal axial mesoderm is delayed during gastrulation.

In overall, these results indicate that the blockade of Delta-1 signaling expanded the mesoendodermal lineage at the expense of the neural ectoderm, while the general blockade of Notch signaling with Notch Mo expanded the mesodermal lineage at the expense of the endoderm and the neural ectoderm. In conclusion, our results show that Notch signaling is involved in the segregation of the three germ layers during gastrulation. They also point to a delicate regulation of this refinement step by Notch ligands and/or non-canonical components of the pathway. Moreover, Notch activity must be finely regulated in order to keep morphogenetic movements at their normal pace during gastrulation.

Effects of blocking Delta-Notch signaling on neural and paraxial mesoderm markers at late gastrula and neural plate stages

It has been described that blocking CSL-dependent Notch signaling at early gastrula leads to an expansion of the expression domain of mesodermal markers and to a reduction of endodermal markers at late neurula, tailbud and tadpole stages (Contakos et al., 2005). We wanted to know if the complementary changes between neural and mesodermal markers that we observed at gastrula stages after blocking Delta-Notch signaling by different means persisted later on development.

When CSL-dependent signaling was impaired by *su(H)1^{DBM}* mRNA injections and early neurulae were analyzed, a mild tendency to increase the paraxial mesoderm markers *myf5* and *myoD* and to decrease the neural marker *sox2* was perceived (Table 1). Supplementary Fig. 3 shows examples of the strongest phenotypes, some of which were selected for histological sections. Double ISH of *sox2* and *myf5* revealed a medio-lateral reduction of the neural plate size and an increase of *myf5* expression (Supplementary Fig. 3A, B). Transverse sections of these embryos and of other specimens hybridized with *myoD* or *sox2* probes revealed an expansion of the paraxial mesoderm in thickness (Table 1; Supplementary Fig. 3B′, D) or in the medio-lateral breadth (Table 1; Supplementary Fig. 3A′, C), while the neural ectoderm was reduced in the medio-lateral axis in a considerable proportion of embryos and was thinner in some specimens (Table 1; Supplementary Fig. 3B′, E). We often observed an increase in the levels of *myoD* transcripts in the paraxial mesoderm in embryos injected with *su(H)1^{DBM}* mRNA (Table 1).

The phenotypes were more consistent when Delta-1 signaling was impaired (Table 1, Figs. 6A–F′) or after a general blockade of the Notch pathway (Table 1, Figs. 6G–L). *Delta-1^{STU}* mRNA injections resulted in an expansion of the *myf5* and *myoD* markers and/or an increase of their intensity on the injected side (Table 1, Figs. 6A, B), while the neural plate, as judged by the expression of *sox2*, was significantly reduced in size (Table 1, Fig. 6C). Transverse sections of these embryos confirm that the paraxial mesoderm is expanded (Figs. 6D–E′ and inset in Fig. 6A), while the neural plate is reduced in the medio-lateral axis (Figs. 6F, F′). In the caudal region of the embryo, surrounding the neurenteric canal, the paraxial mesoderm forms a mesenchyme, with no apparent organization in cell layers, as shown by nuclear Hoescht

staining (Fig. 6D′), but a difference in the intensity of *myf5* expression is already present on the non-injected side, with higher levels in the prospective dorsal layer (Fig. 6D, left side). Interestingly, we observe an increase of *myf5+* cells in the prospective dorsal layer of the paraxial mesoderm on the *delta-1*^{STU}-injected side (inset in Fig. 6A; green arrow in Fig. 6D). At more anterior levels, the paraxial mesoderm is organized in two layers (Fig. 6E′), and *myoD* expression reveals an expansion of the paraxial mesoderm, preferentially of the dorsal layer on the *delta-1*^{STU}-injected side (green arrow in Fig. 6E), while the overlying neural ectoderm is thinner than on the non-

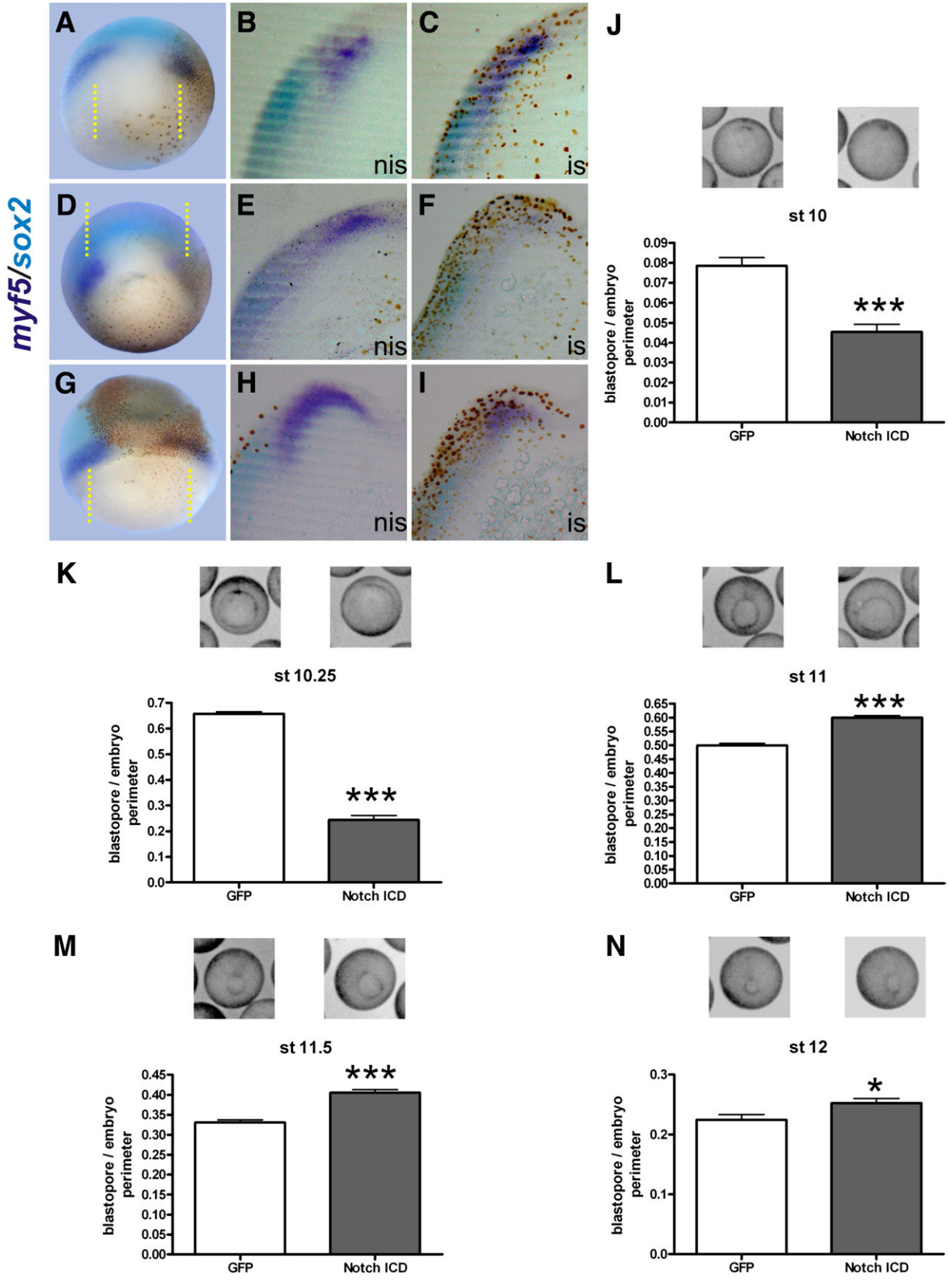

Table 3
Activating Notch signaling impairs gastrulation movements.

Exp No.	Stage	*notch*^{ICD} mean ± sem; *n*	*GFP* mean ± sem; *n*	Difference between means
1	10	0.045 ± 0.004; *n* = 49	0.079 ± 0.004; *n* = 46	***p<0.0001
	10.25	0.24 ± 0.02; *n* = 47	0.657 ± 0.008; *n* = 42	***p<0.0001
	11	0.600 ± 0.008; *n* = 49	0.500 ± 0.007; *n* = 45	***p<0.0001
	11.5	0.405 ± 0.007; *n* = 50	0.331 ± 0.007; *n* = 44	***p<0.0001
	12	0.252 ± 0.008; *n* = 50	0.224 ± 0.008; *n* = 44	*p<0.05
2	10.25	0.8167 ± 0.007; *n* = 32	0.7366 ± 0.0006; *n* = 18	***p<0.0001
	10.5	0.75 ± 0.01; *n* = 26	0.605 ± 0.007; *n* = 17	***p<0.0001
	11.5	0.61 ± 0.02; *n* = 29	0.46 ± 0.02; *n* = 18	***p<0.0001
	12	0.41 ± 0.28; *n* = 29	0.28 ± 0.01; *n* = 16	***p<0.0001

Wild type embryos of the same batch were injected at the 1-cell stage with 1 ng of *notch*^{ICD} + 1 ng of *GFP* mRNA as tracer or 2 ng of *GFP* mRNA (as negative control). Experiment No. 1 and No. 2 were carried out with embryos derived from eggs of two different females. The vegetal hemispheres were scanned at different times during gastrulation. The stage was assigned according to the morphology of the negative controls. The ratio between the perimeter of the blastopores and the perimeter of embryos was calculated as the indicator in the progression of gastrulation. A two-tailed *t*-test was employed to analyze the significance in the difference of the means. The blastopore was significantly larger in embryos injected with *notch*^{ICD} mRNA throughout gastrulation and its formation was delayed at the initial stages.

injected side (Figs. 6E, E′). These results confirm that the dorsal layer of the paraxial mesoderm is particularly sensitive to the levels of Notch activity.

Embryos injected with Notch-Mo fixed when sibling controls reached stage 14 or 15 showed an intriguing situation. While ISH of *myoD* revealed a clear increase in the levels of transcripts and a medio-lateral expansion of the paraxial mesoderm (Fig. 6H), which was confirmed by transverse sections (Figs. 6I, I′), the neural plate was expanded, as judged by the expression of *sox2* (Figs. 6K, L), although it does not seem to be increased at the same extent as after Notch activation. Therefore, we analyzed embryos at an earlier stage (late gastrula). When sibling controls reached stages 12–12.5, Notch Mo-injected embryos showed a notable increase of *myoD* expression (Table 1, Fig. 6G), while the neural plate was greatly reduced in size, as revealed by *sox2* expression (Table 1, Fig. 6J). Interestingly, when embryos were fixed at an intermediate stage (when sibling controls reached stages 12.5–13), there was not a clear tendency regarding to *sox2* expression (Table 1), suggesting that around the end of gastrulation arises an additional hierarchical step controlled by Notch signaling that affects neural development. Embryos injected with Control Mo did not show significant alterations in the patterns of *myoD* or *sox2* in either situation (Table 1).

Overall, these results indicate that after blocking Delta-1 or Notch signaling, the complementary changes between neural and paraxial mesoderm observed at early/mid gastrula stage persist until the end of gastrulation. Afterwards, the expansion of the paraxial mesoderm is maintained at neurula stages, but the neural plate regains its size or is expanded. Other ligand for the Notch receptor and/or a non-canonical Notch-dependent mechanism may be contributing to this neural effect, since it is only observed in Notch Mo-injected embryos.

Discussion

Notch signaling refines the segregation between germ layers in Xenopus

We have previously described that Delta-Notch signaling is involved in the building of the embryonic dorsal midline in *X. laevis*, favoring floor plate against notochord development (López et al., 2003, 2005). Now, we studied if this pathway plays a more general role in the formation of germ layers and obtained evidence that it is involved in refining the segregation between the neural ectoderm, the mesoderm and the endoderm (Fig. 7).

When we activated Notch in the marginal zone, both the suprablastoporal endoderm and the neural ectoderm precursors were expanded, leaving a thinner mesodermal ring around the blastopore (Fig. 7A, left). This is correlated with a thicker and broader neural plate and a thinner paraxial mesoderm at early neurula (our results) and with the expansion of endodermal markers from neurula stage onwards (Contakos et al., 2005). However, when the recombinant Notch^{ICD} protein was distributed more animally at gastrula stage, we observed an expansion of the *bra* domain, although with lower levels of transcripts of the pan-mesodermal marker on the injected side. This expansion is probably the result of a delay in the loss of competence of the ectoderm in response to mesodermal inducers, as has been previously reported by other authors who used the notch ΔE construct in animal cap assays (Coffman et al., 1993; Abe et al., 2004). Thus, depending on the distribution of the Notch^{ICD} recombinant protein, expansions or reductions of the mesoderm should be expected, and this may in part explain the contradictory results of Notch effects on mesoderm that were reported elsewhere at later stages of development.

While the effects on ectoderm and animal caps, which normally do not give rise to mesoderm, may reflect ectopic activations of Notch, we are more interested on the function of Delta-Notch in the marginal zone, from where the mesoderm arises. Besides, this seems to represent more accurately what happens at normal development at the beginning of gastrulation, when Notch ligands are first detectable by ISH in a ring around the blastopore.

Supporting this idea, the effects of blocking Delta-Notch signaling were confined around the marginal zone for the three markers of germ layers analyzed. We observed a consistent expansion of the *bra* domain and an animal shift of the neural border, while the suprablastoral endoderm was either expanded if Delta-1 signaling was blocked (Fig. 7A, center), or reduced after a general knock-down of Notch (Fig. 7A, right).

These phenotypes demonstrate that Delta-Notch signaling is involved in the segregation of the three germ layers during gastrulation. As depicted in the model proposed in Fig. 7B, this may be accomplished at two levels:

(A) By refining the limit of involution between the mesoendodermal cells in the involuting marginal zone and the ectoderm in the non-involuting marginal zone. This is supported by the fact that active Notch moves the limit vegetalwards, and blocking Delta1-Notch signaling moves it animalwards (type A decisions, yellow pathway in Fig. 7B).

Fig. 3. Notch^{ICD} alters the expression domain of *myf5* and impairs morphogenetic movements during gastrulation. (A–I) Embryos were injected with 1 ng of *notch*^{ICD} mRNA in one cell at the 2- or 4-cell stage and fixed when sibling controls reached stage 11. They were revealed by ISH with *myf5* (purple staining) and *sox2* probes (turquoise staining). Dorsal–vegetal views of whole embryos (A,D,G) and a corresponding pair of contralateral parasagittal sections (B,C; E,F; H,I, respectively) are shown, to compare changes between the injected- (is) and the non-injected- (nis) sides. The blastopore is at the upper right angle on the sections. Yellow dotted lines in (A,D,G) indicate the planes of the sections. Brown dots correspond to immunolocalization of the Myc-tag epitope fused to Notch^{ICD}. Although the BCIP staining (turquoise) is not as sensitive as the NBT + BCIP staining, it is possible to observe that the *sox2* domain is shifted towards the blastopore on the injected side in the embryo shown in (A). (J–N) Wild type sibling embryos were injected with 1 ng of *notch*^{ICD} + 1 ng of *GFP* mRNA as tracer or with 2 ng of *GFP* mRNA as negative control at the 1-cell stage. The progress of the blastopore was recorded through gastrulation by scanning the vegetal sides at stage 10 (J), 10.25 (K), 11 (L), 11.5 (M) and 12 (N). Data are represented as the ratio between the perimeter of the blastopore and the embryo's perimeter in *notch*^{ICD}- (gray bars) and *GFP*- (white bars) injected embryos. Bars represent mean ± sem. An embryo illustrating the mean of the group is shown above each bar. Notice that at early gastrula, the relative perimeter of the blastopore is lower in *notch*^{ICD}-injected embryos than in *GFP*-injected siblings because of the delay in the appearance and progress of the slit, which is shorter in the former group. At later stages, when the slit depicts a full circumference, the blastopores are larger in *notch*^{ICD}-injected embryos and thus, the relative perimeter of the blastopore is higher than in GFP-injected siblings, also reflecting a delay in its progress. For additional details, see legend to Table 3. This figure illustrates experiment No. 1.

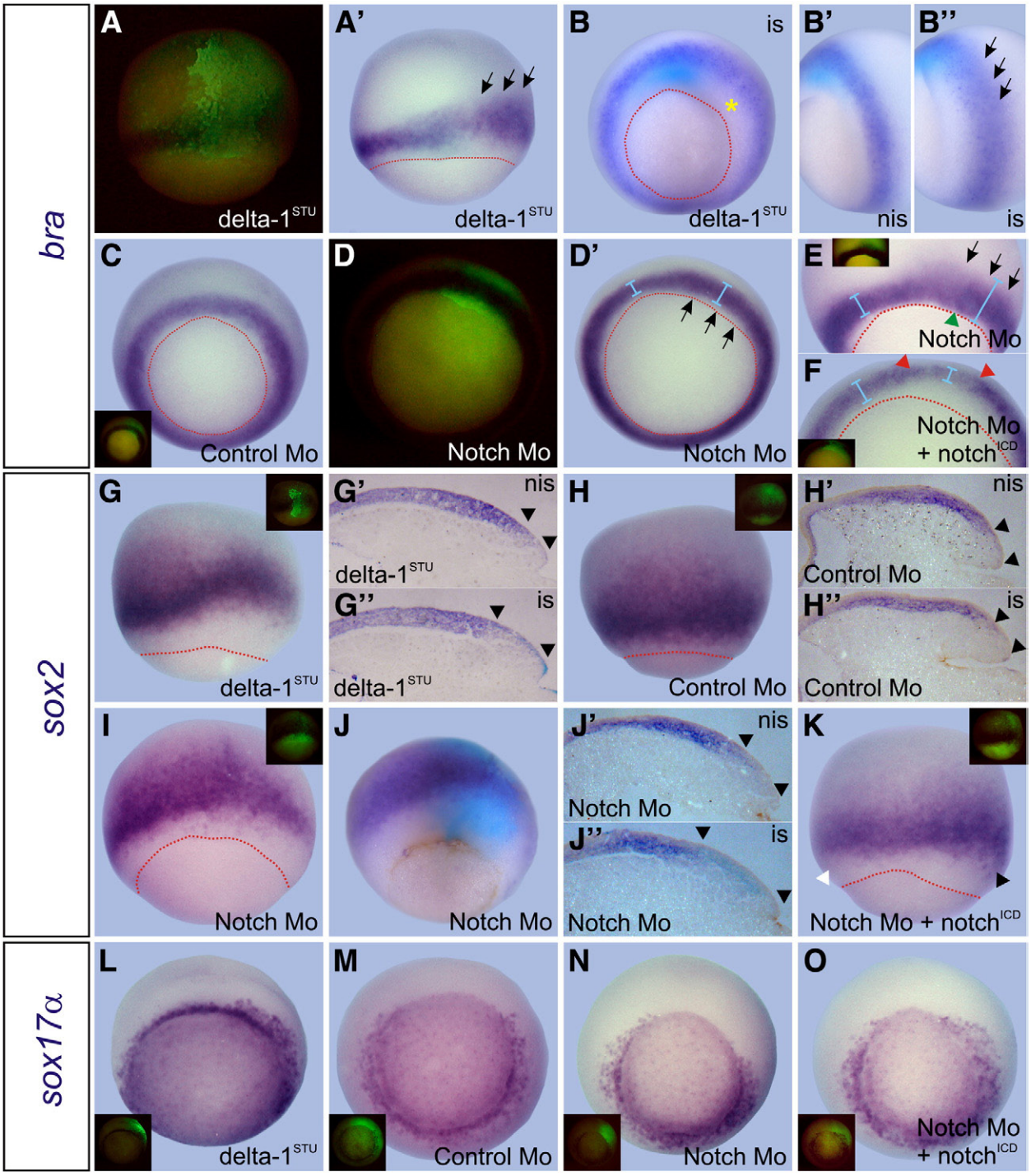

Fig. 4. Blocking Notch signaling produces complementary changes in the expression of markers of the three germ layers at gastrula. Embryos were injected in one cell at the 4-cell stage with 1 ng of *delta*^{STU} mRNA (A–B″,G–G″,L), 20 ng of Control morpholino (Control Mo; C,H–H″,M), 20 ng of Notch Mo (D–E,I–J″,N), or with 20 ng of Notch Mo + 1 ng of *notch*^{ICD} mRNA (F,K,O). They were fixed when sibling control embryos reached stage 11 and were revealed by ISH with the following probes: *bra* (purple staining, A–F), *sox2* (purple staining, G–K), *sox17α* (purple staining, L–O). When possible, embryos hybridized with *bra* were also revealed with a *chd* probe to readily identify the dorsal side (turquoise staining in A′–B″). All photographs of whole embryos were oriented with the injected side towards the right. is: injected side; nis: non-injected side. Dotted red lines delineate the blastopore. Embryos are shown with the corresponding fluorescence image at the left (A,D for A′,D′, respectively) or in the insets, to identify the injected side (green fluorescence), which was revealed by immunofluorescence of GFP (A,G,L), DOG (C,D,E,H,I,M,N) or the Myc-tag epitope fused to Notch^{ICD} (F,K,O). (B,C–D′,L–O) Vegetal views, with the dorsal side up. (A,A′,E,G,H,I,J,K) Dorsal views. (B′,B″) Lateral views of the non-injected- and the injected side, respectively, of the embryo shown in (B). In this case, photographs were inverted to facilitate comparisons between both sides. This embryo was co-injected with 1 ng of GFP mRNA as tracer, and the injected side was determined by the fluorescence of GFP before the ISH procedure. (D,D′ and E) Two different embryos injected with Notch Mo. (G′,G″) Contralateral parasagittal sections of an embryo injected with *delta-1*^{STU} mRNA + BDA as tracer, which was revealed with BCIP (turquoise staining). (H′,H″) Contralateral parasagittal sections of the embryo injected with Control Mo shown in (H). (J′,J″) Contralateral parasagittal sections of the embryo shown in (J), which was injected with Notch Mo and revealed by immunostaining of the fluorescein epitope with BCIP (turquoise staining). Arrows in (A′,B″,E) point to the animal expansion of the *bra* domain. The asterisk in (B) indicates an expansion of the gap of unstained cells between the *bra*+ ring and the blastopore, which correlates with an expansion of the suprablastoporal endoderm (see L for comparison). Arrows in (D′) and the green arrowhead in (E) point to the vegetal expansion of the *bra* domain. Light blue bars in (D′,E,F) indicate the difference in the width of the *bra* domain between the injected- and the non-injected side. Notice the stretch of thinner and lower *bra* staining between the red arrowheads in (F), coinciding with the green fluorescence on the *bra* domain on the inset, indicating that *notch*^{ICD} reversed the effect of Notch Mo. The black arrowheads in (G′,G″,H′,H″,J′,J″) indicate the distance between the blastopore and the vegetal border of the *sox2* domain. The black arrowhead in (K) points to supernumerary *sox2*+ cells in the marginal zone on the injected side that are not present on the non-injected side (white arrowhead), indicating that *notch*^{ICD} mRNA reversed the effect of Notch Mo on the location of the vegetal boundary of *sox2*.

Table 4
Blocking Notch signaling impairs gastrulation movements.

Exp No.	Stage	Notch Mo mean ± sem; n	Control Mo mean ± sem; n	Difference between means
1	10	0.064 ± 0.006; $n=41$	0.059 ± 0.005; $n=38$	ns, $p>0.05$
	10.25	0.673 ± 0.009; $n=41$	0.65 ± 0.01; $n=34$	ns, $p>0.05$
	11	0.519 ± 0.008; $n=41$	0.499 ± 0.008; $n=34$	ns, $p>0.05$
	11.5	0.3667 ± 0.006; $n=41$	0.346 ± 0.006; $n=34$	*$p<0.05$
	12	0.242 ± 0.005; $n=40$	0.221 ± 0.006; $n=30$	**$p<0.01$
2	10.25	0.75 ± 0.01; $n=14$	0.69 ± 0.01; $n=9$	**$p<0.01$
	10.5	0.63 ± 0.01; $n=13$	0.56 ± 0.02; $n=9$	**$p<0.01$
	11.5	0.48 ± 0.02; $n=13$	0.43 ± 0.02; $n=10$	ns, $p>0.05$
	12	0.31 ± 0.02; $n=14$	0.30 ± 0.04; $n=11$	ns, $p>0.05$

Wild type embryos of the same batch were injected at the 1-cell stage with 20 ng of Notch Mo or 20 ng of Control Mo. Experiment No. 1 and No. 2 were carried out with embryos derived from eggs of two different females. The vegetal hemispheres were scanned at different times during gastrulation. The stage was assigned according to the morphology of the Control Mo-injected embryos. The ratio between the perimeter of the blastopores and the perimeter of embryos was calculated as the indicator in the progression of gastrulation. A two-tailed *t*-test was employed to analyze the significance in the difference of the means. A significant delay in the progress of the blastopore was detected at some stages during gastrulation in embryos injected with Notch Mo (* and **). ns: non-significative differences.

(B) By refining the segregation between mesoderm and endoderm within the involuting marginal zone. This is supported by the observation that active Notch favors endoderm development at the expense of mesoderm, while the general blockade of Notch signaling gives the opposite result (type B decisions, light blue pathway in Fig. 7B).

Strikingly, blocking Delta-1 signaling only moves the limit of involution, favoring mesoendodermal development at the expense of the neural ectoderm. This suggests that Delta-1 is the ligand responsible of type A decisions and raises questions about the nature of the ligand and the down-stream mechanisms involved in mesodermal vs. endodermal decisions (type B), which were only revealed by Notch Mo.

Although we did not assay specific markers, we presume that the entire ectoderm undergoes the effects manifested by the neural ectoderm, since we also observed expansions of *sox17α* or *bra* in more ventral locations around the blastopore after manipulating Delta-Notch signaling. Moreover, the non-neural ectoderm was thicker on the injected side in *notch^{ICD}*-injected neurulae (not shown).

At the gastrula stages that we analyzed, the *sox17α* domain is juxtaposed to the blastopore, while the *bra* domain forms a ring between the *sox17α* and *sox2* domains. After Delta-Notch manipulations, we observed displacements of the boundaries between them rather than changes in the density of cells expressing either marker within the domains (Fig. 4, Table 2), which should be expected if a lateral inhibition process is being altered. However, lateral inhibition could be involved at the borders of the germ layers when cell fates are not yet decided, in order to refine the patterns of gene expression to conform to their position. In fact, we noticed that, normally, the three markers analyzed show more diffuse patterns of expression or more scattering of cells expressing the marker at the borders of juxtaposition (Fig. 4), suggesting some intermingling of germ layers. Indeed, single cell RT-PCR analysis demonstrated that at early gastrula, individual cells at the marginal zone may express markers of two or even the three germ layers in *Xenopus*, but become progressively and asynchronously committed to one germ layer during gastrulation (Wardle and Smith, 2004). Alternatively, another possibility that should be considered is the role of Notch signaling in the establishment of boundaries between fields of cells that are segregating in the marginal zone, including the limit of involution (Bray, 1998, 2006). Interestingly, we have found that Serrate, which together with Delta is involved in the establishment of the dorsal–ventral boundary of the wing imaginal disc in flies (Lai, 2004; Fortini, 2009), is expressed around the blastopore in the *Xenopus* gastrula (unpublished results).

To discern between these possibilities, studies at the single cell level should be addressed, while manipulating Notch and its ligands, at the time when the germ layers are being specified and segregated.

The observation that Notch favors endoderm but disfavors mesoderm development in *Xenopus* is supported by another report (Contakos et al., 2005). These authors show that the activation of Notch signaling at the beginning of gastrulation leads to an increase of many endodermal markers at later stages of development, whereas markers of paraxial, lateral plate and intermediate mesoderm decreased their expression. Blocking CSL-dependent Notch signaling at gastrulation produced the opposite results. This evidence supports the role of Notch signaling in subdividing germ layers during gastrulation.

Although these authors claim that Notch activation leads to an expansion of markers of endodermal tissues at the expense of mesodermal cell types, they favor a delay in the differentiation of mesoderm rather than a binary cell fate choice between endodermal and mesodermal fates to explain their results. This conclusion is difficult to interpret and was based on lineage labeling observations demonstrating that cells with active Notch signaling were detected throughout the three germ layers, including the mesoderm. However, it is unlikely that a delay in differentiation explains the persistent decrease of mesodermal markers throughout all the stages examined (from neurula to tadpole). Moreover, we observed that not all the mesodermal cells respond uniformly to Notch activation, and this seems to be correlated with their dorsal/ventral allocation within the paraxial mesoderm, the dorsal cells being more sensitive to Notch activation than the ventral ones. Supporting this, when Delta-1 was blocked, the dorsal layer was preferentially expanded.

Strikingly, it has been described that at the early neurula stage, the prospective somitic cells form two layers of cuboidal cells, separated by an interface. Eventually, as neurulation proceeds, an asymmetry arises in the behavior of the cells in their shaping and fates above and below the interface. This asymmetry results in an array of elongated cells which are thought to become the myotome, and a thin layer of cuboidal cells that presumably gives rise to the dermatome (Keller, 2000). It will be interesting to investigate in the future whether the differential response to Notch signaling that we observe between both layers in the paraxial mesoderm at early neurula is related to the asymmetry of behaviors suggested by Keller and if they differ in their potential to become neural tissue if Notch signaling is activated.

Possible mechanisms involved in Notch-mediated segregation of germ layers

Specific molecular manipulations have been previously shown to change the specification of germ layers in *Xenopus*. For example, a *bra* mutant truncated in the C-terminus, which antagonizes *bra* activity, can neuralize animal cap explants instead of inducing mesoderm, as the wild type protein does (Rao, 1994). LIM domain mutants of the transcription factor *Xlim-1* are able to neuralize animal cap explants, but when co-expressed with *bra* they induce mesoderm, instead (Taira et al., 1994). Moreover, experiments conducted in the whole embryo show that changing germ layer specification dramatically affects gastrulation movements. For example, overexpression of the endodermal marker *gata5* respecifies ectoderm and mesoderm towards endoderm and disrupts the blastopore closure (Weber et al., 2000). Blocking *sox3* activity leads to major gastrulation defects and to an animalward expansion of mesendodermal and mesodermal markers. (Zhang et al., 2004).

Increasing or decreasing the activity of Notch impairs morphogenetic movements but do not stop gastrulation, indicating that the three germ layers are formed. However, they do not develop normally at later stages, and it will be interesting to evaluate which are the

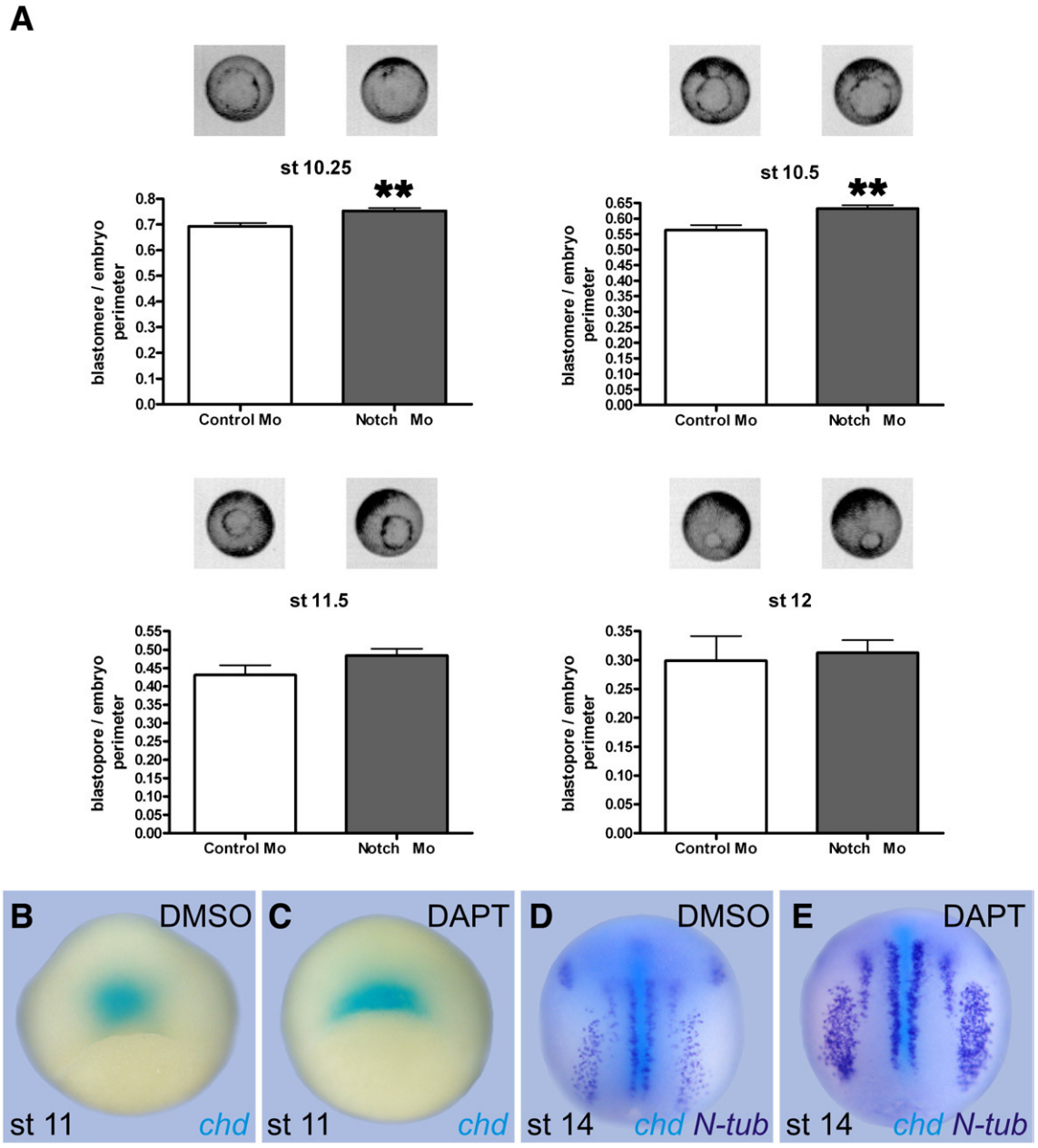

Fig. 5. Blocking Notch signaling impairs morphogenetic movements during gastrulation. (A) Wild type embryos of the same batch and derived from eggs of the same female were injected with 20 ng of Control Mo or with 20 ng of Notch Mo before the first mitotic division. The progress of the blastopore was recorded through gastrulation by scanning the vegetal sides at stages 10.25, 10.5, 11.5 and 12. Data are represented as the ratio between the perimeter of the blastopore and the embryo's perimeter in Notch Mo- (gray bars) and Control Mo- (white bars) injected embryos. Above each bar, an embryo representing the mean of the group is shown. For additional details, see legend to Table 4. This figure illustrates experiment No. 2. (B–E) Embryos of the same batch and derived from eggs of the same female were treated from the 1-cell stage with 100 μM of the γ-secretase inhibitor DAPT or with vehicle alone (DMSO) and fixed at stage 11 (B,C) for ISH of *chd* (turquoise staining) or at stage 14 for ISH of *chd* (turquoise staining) and *N-tubulin* (*N-tub*, purple staining).

consequences of impairing the gastrulation movements in their ulterior patterning. Since there is not a complete transformation of one germ layer into another and some cells are refractory to the manipulation of the level of Notch activity, this pathway is not essential for the formation of the germ layers in *Xenopus*, but rather works in refining the limits between them during their segregation.

Although CSL-dependent signaling may contribute to this process, non-canonical signaling seems to be involved, because the effects of $su(H)1^{DBM}$ were mild or without a clear tendency, while $delta\text{-}1^{STU}$ or Notch Mo always gave consistent results. The Notch Mo phenotype was reversed by $Notch^{ICD}$, suggesting that at least, the intracellular domain of the Notch receptor is involved in this process. However, this does not mean that CSL participates, since $Notch^{ICD}$ has been shown to regulate some target genes independently of CSL in some contexts (Hu et al., 2006). Alternatively, the milder phenotype observed with $su(H)1^{DBM}$ may be reflecting the canceling effects of blocking both the repressor and activator functions of Su(H), as it has been suggested before for CSL mutations (Lai, 2004).

Nodal signaling is necessary for both endoderm and mesoderm induction in *Xenopus*. A gradient of Nodal activity may be involved in separating mesoderm from endoderm, with highest levels inducing the latter (Kimelman and Griffin, 2000). Moreover, it has been proposed a gene regulatory network that operates in the animal–vegetal axis, where a Sox code establishes germ layer specification by repressing or activating Nodal signaling at multiple levels (Zhang and Klymkowsky, 2007). In the animal hemisphere, maternal *sox3* (B1-

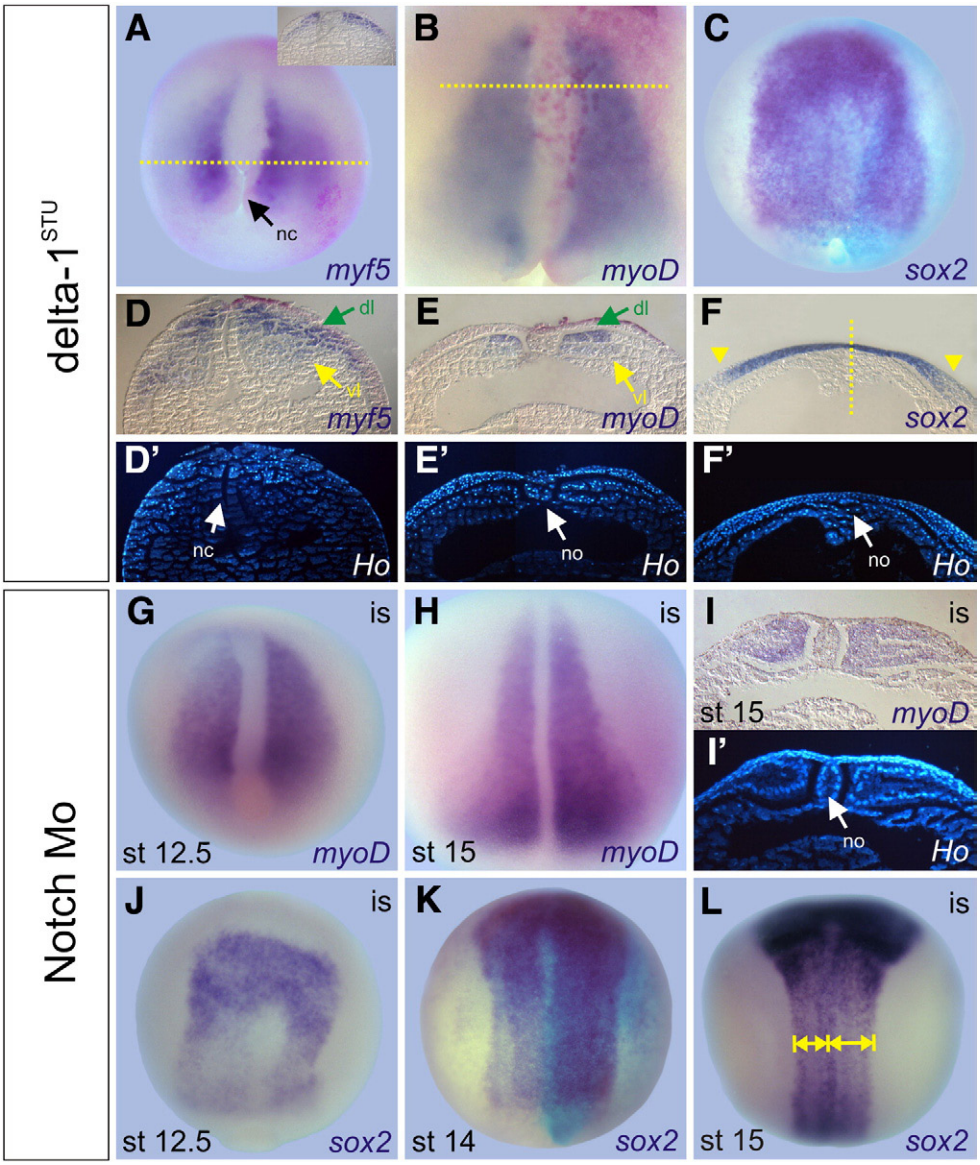

Fig. 6. Effects of blocking Notch signaling on neural and paraxial mesodermal markers at the late gastrula and neural plate stage. Embryos were injected in one cell at the 4-cell stage with 0.5 ng of *delta-1*^{STU} mRNA (A,B,D,D′,E,E′), 1 ng of *delta-1*^{STU} mRNA (C,F,F′) or 20 ng of Notch Mo (G–L). They were fixed when sibling controls reached stage 12.5 (G,J), 14 (A–F,K) or 15 (H,I,I′,L) and were revealed by ISH of *myf5* (purple staining in A,D), *myoD* (purple staining in B,E,G,H,I) or *sox2* (purple staining in C,F,J–L). Embryos injected with *delta-1*^{STU} mRNA and the embryo shown in (K) were co-injected with BDA as tracer, which was revealed after a chromogenic reaction with Magenta Phos (A,B,D,E) or BCIP (turquoise staining, C,F,K). In the rest of the embryos, the injected side was determined by the fluorescence of the morpholino before the ISH procedure. Whole embryos are shown in dorsal views, anterior up, except in (A), which shows a dorsal-posterior view. All photographs were oriented with the injected side towards the right. The horizontal yellow dotted lines in (A,B) show the plane of transverse sections shown in the inset in (A) and in the photograph in (E), respectively. (D,D′) Transverse section at the level of the neurenteric canal of an embryo similar to the one shown in (A). (I) Transverse section at the mid-trunk level of an embryo similar to the one shown in (H). (D′,E′,F′,I′) Nuclear Hoescht staining of the sections shown in (D,E,F,I), respectively. Green arrow in (D): prospective dorsal layer (dl) of the paraxial mesoderm. Yellow arrow in (D): prospective ventral layer (vl) of the paraxial mesoderm. Green arrow in (E): dorsal layer (dl) of the paraxial mesoderm. Yellow arrow in (E): ventral layer (vl) of the paraxial mesoderm. nc: neurenteric canal; no: notochord. The vertical yellow dotted line in F depicts the embryo's midline, and yellow arrowheads point to the lateral borders of the *sox2* domain, showing the reduction of the neural plate on the medio-lateral axis on the injected side. Double arrows in (L) show the difference in the width of the *sox2* domain between the injected- and the non-injected side.

type) inhibits Nodal signaling both directly, by reducing *Xnr5* and *Xnr6* RNA levels, and indirectly, through the up-regulation of zygotically expressed genes which, in turn, inhibit the effects of secreted Nodal proteins. This animal program ultimately leads to ectoderm and neuroectoderm specification. In the vegetal hemisphere, on the other side, maternal *sox7* (F-type) is thought to promote Nodal signaling as well as the expression of several genes associated with mesodermal and endodermal differentiation, including *sox17*, which is also up-regulated by Nodal.

Strikingly, we have shown that Delta-Notch signaling modifies the expression of at least one B1-type sox gene (*sox2*) and one F-type sox gene (*sox17α*), suggesting that this pathway could be refining the segregation of germ layers through the modulation of the Sox code that is established in the animal–vegetal axis. Future prospects include studying how Notch and its ligands modify the expression of the genes involved in the regulatory network controlled by Sox proteins and Nodal signaling. It will be interesting to test if Notch can modify the response of the marginal zone cells to Nodal during the segregation of the germ layers. For instance, Notch has been shown to prolong the period of competence of animal caps to respond to mesodermal inducers (Coffman et al., 1993; Abe et al., 2004).

The overlapping expression patterns of *bra*, *myoD* and *delta* in the marginal zone during gastrulation and its functional significance are intriguing. *Bra* transcripts are found in the pre-involuted and in the

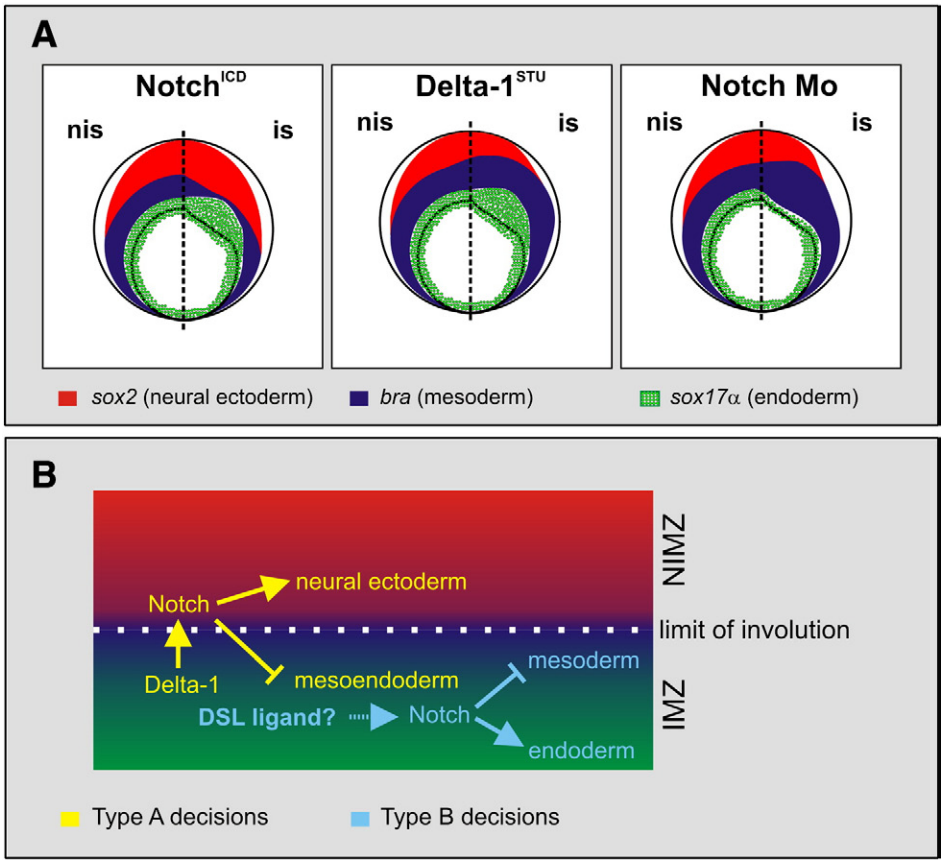

Fig. 7. Schematic model summarizing the phenotypes after manipulating Delta-Notch signaling (A) and the role of this pathway on the segregation of the three germ layers in *Xenopus* embryos (B). (A) Diagram of gastrula embryos at stages 10.5–11 showing the expression pattern of the neural marker *sox2* (red), the pan-mesodermal marker *bra* (blue) and the endodermal marker *sox17α* (green) in embryos injected with *notch*^{ICD} mRNA, *delta-1*^{STU} mRNA and Notch Mo. The dorsal region is up, ventral is down. The left side represents the non-injected side (nis), and the right side, the injected side (is). (B) Diagram summarizing the proposed model for the role of Delta-Notch signaling in the marginal zone. IMZ: involuting marginal zone. NIMZ: non involuting marginal zone. The dotted white line represents the limit of involution. Neural ectoderm is in red, mesoderm in blue, endoderm in green. See text for details.

recently involuted mesoderm. When this layer extends towards the anterior region of the embryo, *bra* is down-regulated in all mesodermal derivatives with the exception of the notochord and the circumblastoporal collar. On the other hand, *delta-1* transcripts are present in the pre-involuted mesoderm but disappear during involution, while the expression of *myoD*, which is induced in the marginal zone in the presumptive mesodermal cells around the onset of gastrulation, persists after involution (Wittenberger et al., 1999). Interestingly, these authors described that *myoD* directly up-regulates *delta-1* and is able to activate Notch signaling. Together with our results, this suggests that once mesoderm is induced, the transient activation of *delta-1* by *myoD* may be establishing a feed-back loop involving Notch activity that further limits the number of mesodermal cells during the segregation of the germ layers.

Comparison with other models and evolutive implications

In zebrafish embryos, activating Notch signaling during early development results in a reduction in the number of endodermal cells and there is indirect evidence that it also favors somitic development, suggesting that Notch might play a role in the segregation of mesoderm from endoderm. However, none of the strategies employed to block Notch signaling resulted in the opposite effects, although the morpholino approach was not used to knock-down the receptor (Kikuchi et al., 2004). In sea urchins, activation of Notch signaling increases mesodermal precursors, reduces the number of presumptive endoderm cells and shifts the ectoderm–endoderm boundary animalwards, while the opposite changes take place when Notch signaling is inhibited (Sherwood and McClay, 1999, 2001).

It is surprising that after manipulating Notch signaling, the three germ layers respond in the opposite way in *Xenopus* when compared to sea urchin and zebrafish embryos. Indeed, the general blockade of the pathway with *Xenopus* Notch Mo strikingly gives the same results than activating Notch in sea urchin. However, other evidence from Metazoans suggests that Notch is able to promote ectodermal or neural development at the expense of the mesoderm, reminding our observations in *Xenopus*.

In the spider, for example, the posterior half of the body is formed as the result of growth of the domain surrounding the blastopore, and Delta transcription is activated in some cells which are allowed to become mesoderm. Notch is in turn activated in neighboring cells, which are prevented from adopting a mesodermal fate while being instructed towards a caudal ectoderm fate (Oda et al., 2007; Oda and Akiyama-Oda, 2008). In addition, in vitro analysis showed that Notch blocks mesodermal differentiation at the initial stages of embryonic stem cells differentiation and promotes neural commitment when these cells are cultured in the absence of self renewal and serum factors, suggesting that Notch plays a role during the specification of the germ layers during mammalian embryogenesis (Schroeder et al., 2006; Lowell et al., 2006). Moreover, during the initial stages of embryogenesis in nematodes, cells respond to Notch activation either remaining as ectodermal precursors or becoming mesodermal precursors. This depends on complex cell–cell interactions that occur through early cleavage stages, according to when and where the new cells are born (Good et al., 2004).

Although it is difficult to reconcile the results between *Xenopus* and zebrafish, several factors could contribute to these discrepancies. There are a number of differences in the early development between both species, including aspects in the molecular cascades leading to mesendoderm specification, such as Nodal and VegT requirements (reviewed by Kimelman and Griffin, 2000; Shivdasani, 2002).

In zebrafish, the endoderm arises from a small band closest to the margin of the blastula and mesoderm, from a wider band. Unlike in *Xenopus*, the vegetal hemisphere consists of the extra-embryonic yolk cell and the associated yolk syncytial layer, which do not contribute to the endoderm. Thus, the majority of endodermal and mesodermal progenitors are intermingled at the margin rather than being separated along the equator and the vegetal hemisphere, as occurs in *Xenopus* (Kimelman and Griffin, 2000).

In zebrafish, *sox17* down-regulation by Notch was observed at the 80% epiboly stage (i.e. on the second half of gastrulation), while our results were analyzed on the first half of gastrulation. We do not know if this is relevant to explain our differences, but it is known that Notch signaling can elicit opposite effects on different germ layers derivatives depending on time (Glavic et al., 2004; Contakos et al., 2005). For instance, we found that the effects of decreasing Delta-Notch signaling that we observe at the beginning of gastrulation are still evident at the end of this process, but afterwards, an opposite effect begins to emerge in the neural plate. This suggests that a novel point of Notch-dependent regulation in the development of the neural ectoderm arises at the beginning of neurulation, when a non-canonical mechanism and/or another ligand distinct from Delta-1 may contribute to regulate the size of the neural plate. Interestingly, the overexpression of the non-canonical component Deltex in *Xenopus* leads to an expansion of the neural ectoderm (Kishi et al., 2001).

All these data suggest that, notwithstanding the different outcomes on cell fates, Notch signaling has been used throughout evolution in the animal kingdom to specify alternative fates in germ layers or contributing to their segregation. It will be interesting to acknowledge if the changing patterns of cell–cell interactions in space and time or different contributions of other mechanisms to germ layer segregation, such as lateral inhibition and boundary formation, underlie the differences observed between species.

In *X. laevis*, the thin monolayer of epithelial cells that covers the involuting marginal zone and expresses *sox17α* constitutes the suprablastoporal prospective endoderm. This layer involutes and is fated to become the endodermal lining of the roof of the archenteron, although a few cells in some, but not in all embryos, become incorporated into somitic and notochordal mesoderm during neurulation (Keller, 2000). The complementary changes in the expression of *bra* and *sox17α* that we observe in the marginal zone after manipulating Notch signaling suggest that this pathway may be involved in stochastic bipotential fate decisions between endoderm and mesoderm that refine the development of this layer. Interestingly, in other anuran species, the prospective somitic mesoderm and notochord occupy large areas in the superficial epithelial layer of the involuting marginal zone (Keller, 2000). This, together with our results, uncovers the potential of this layer to give rise to both mesoderm and endoderm and the different ways of segregation that have arisen through amphibian evolution.

The opposite results of manipulating Notch in Metazoans discussed above suggest that subtle modifications of this pathway may underlie the evolution of different strategies for the segregation of germ layers.

Acknowledgments

We wish to acknowledge the following colleagues for providing us with the constructs for making synthetic mRNA: Thomas Hollemann for *X-notch*^{ICD}, John Gurdon for *GPF*, Chris Kintner for *X-su(H)1*^{DBM}. We are also grateful to the following researchers for providing us with the constructs for making ISH probes: Igor Dawid for *N-tubulin*, Eddy De Robertis for *X-chordin*, Abraham Fainsod for *X-brachyury*, Christof Niehrs for *X-myoD* and *X-myf5*, Yoshiki Sasai for *X-sox2* and Hugh R. Woodland for *X-sox17α*. We also wish to thank Ana Adamo for material support and members of our lab (Helena Acosta, Cecilia Aguirre, Victoria Gnazzo, Sabrina Murgan, Grazielle Pacheco and Cristina Zamorano) for helping with embryos and reagents preparation.

S. L. L. is from CONICET; A. R. P. and A. E. C. are from CONICET and Universidad de Buenos Aires. D. R. R. was supported by a fellowship from ANPCyT. This paper was supported by grants to S. L. L from ANPCYT (BID PICT 767/06) and to A. E. C. from CONICET (PIP 6123/05), ANPCyT (BID PICT 32024/05) and Universidad de Buenos Aires (M803/05).

Appendix A. Supplementary data

Supplementary data associated with this article can be found, in the online version, at doi:10.1016/j.ydbio.2010.01.010.

References

Abe, T., Furue, M., Myoishi, Y., Okamoto, T., Kondow, A., Asashima, M., 2004. Activin-like signaling activates Notch signaling during mesodermal induction. Int. J. Dev. Biol. 48, 327–332.

Benedito, R., Roca, C., Sorensen, I., Adams, S., Gossler, A., Fruttiger, M., Adams, R.H., 2009. The notch ligands Dll4 and Jagged1 have opposing effects on angiogenesis. Cell 137, 1124–1135.

Bray, S., 1998. Notch signalling in Drosophila: three ways to use a pathway. Semin. Cell Dev. Biol. 9, 591–597.

Bray, S.J., 2006. Notch signalling: a simple pathway becomes complex. Nat. Rev. Mol. Cell Biol. 7, 678–689.

Chitnis, A., Henrique, D., Lewis, J., Ish-Horowicz, D., Kintner, C., 1995. Primary neurogenesis in Xenopus embryos regulated by a homologue of the Drosophila neurogenic gene Delta. Nature 375, 761–766.

Coffman, C., Harris, W., Kintner, C., 1990. Xotch, the Xenopus homolog of Drosophila notch. Science 249, 1438–1441.

Coffman, C.R., Skoglund, P., Harris, W.A., Kintner, C.R., 1993. Expression of an extracellular deletion of Xotch diverts cell fate in Xenopus embryos. Cell 73, 659–671.

Contakos, S.P., Gaydos, C.M., Pfeil, E.C., McLaughlin, K.A., 2005. Subdividing the embryo: a role for Notch signaling during germ layer patterning in Xenopus laevis. Dev. Biol. 288, 294–307.

D'Souza, B., Miyamoto, A., Weinmaster, G., 2008. The many facets of Notch ligands. Oncogene 27, 5148–5167.

Dale, L., Slack, J.M., 1987. Fate map for the 32-cell stage of Xenopus laevis. Development 99, 527–551.

Fortini, M.E., 2009. Notch signaling: the core pathway and its posttranslational regulation. Dev. Cell 16, 633–647.

Franco, P.G., Paganelli, A.R., López, S.L., Carrasco, A.E., 1999. Functional association of retinoic acid and hedgehog signaling in Xenopus primary neurogenesis. Development 126, 4257–4265.

Frank, D., Harland, R.M., 1991. Transient expression of XMyoD in non-somitic mesoderm of Xenopus gastrulae. Development 113, 1387–1393.

Glavic, A., Silva, F., Aybar, M.J., Bastidas, F., Mayor, R., 2004. Interplay between Notch signaling and the homeoprotein Xiro1 is required for neural crest induction in Xenopus embryos. Development 131, 347–359.

Good, K., Ciosk, R., Nance, J., Neves, A., Hill, R.J., Priess, J.R., 2004. The T-box transcription factors TBX-37 and TBX-38 link GLP-1/Notch signaling to mesoderm induction in C. elegans embryos. Development 131, 1967–1978.

Hopwood, N.D., Pluck, A., Gurdon, J.B., 1991. Xenopus Myf-5 marks early muscle cells and can activate muscle genes ectopically in early embryos. Development 111, 551–560.

Hori, K., Fostier, M., Ito, M., Fuwa, T.J., Go, M.J., Okano, H., Baron, M., Matsuno, K., 2004. Drosophila deltex mediates suppressor of Hairless-independent and late-endosomal activation of Notch signaling. Development 131, 5527–5537.

Hu, Q.D., Ang, B.T., Karsak, M., Hu, W.P., Cui, X.Y., Duka, T., Takeda, Y., Chia, W., Sankar, N., Ng, Y.K., Ling, E.A., Maciag, T., Small, D., Trifonova, R., Kopan, R., Okano, H., Nakafuku, M., Chiba, S., Hirai, H., Aster, J.C., Schachner, M., Pallen, C.J., Watanabe, K., Xiao, Z.C., 2003. F3/contactin acts as a functional ligand for Notch during oligodendrocyte maturation. Cell 115, 163–175.

Hu, Q.D., Ma, Q.H., Gennarini, G., Xiao, Z.C., 2006. Cross-talk between F3/contactin and Notch at axoglial interface: a role in oligodendrocyte development. Dev. Neurosci. 28, 25–33.

Hudson, C., Clements, D., Friday, R.V., Stott, D., Woodland, H.R., 1997. Xsox17alpha and -beta mediate endoderm formation in Xenopus. Cell 91, 397–405.

Ito, M., Katada, T., Miyatani, S., Kinoshita, T., 2007. XSu(H)2 is an essential factor for gene expression and morphogenesis of the Xenopus gastrula embryo. Int. J. Dev. Biol. 51, 27–36.

Keller, R., 2000. The origin and morphogenesis of amphibian somites. Curr. Top. Dev. Biol. 47, 183–246.

Kikuchi, Y., Verkade, H., Reiter, J.F., Kim, C.H., Chitnis, A.B., Kuroiwa, A., Stainier, D.Y.,

2004. Notch signaling can regulate endoderm formation in zebrafish. Dev. Dyn. 229, 756–762.
Kimelman, D., Griffin, K.J., 2000. Vertebrate mesendoderm induction and patterning. Curr. Opin. Genet. Dev. 10, 350–356.
Kishi, N., Tang, Z., Maeda, Y., Hirai, A., Mo, R., Ito, M., Suzuki, S., Nakao, K., Kinoshita, T., Kadesch, T., Hui, C., Artavanis-Tsakonas, S., Okano, H., Matsuno, K., 2001. Murine homologs of deltex define a novel gene family involved in vertebrate Notch signaling and neurogenesis. Int. J. Dev. Neurosci. 19, 21–35.
Kiyota, T., Jono, H., Kuriyama, S., Hasegawa, K., Miyatani, S., Kinoshita, T., 2001. X-Serrate-1 is involved in primary neurogenesis in Xenopus laevis in a complementary manner with X-Delta-1. Dev. Genes Evol. 211, 367–376.
Kopan, R., Nye, J.S., Weintraub, H., 1994. The intracellular domain of mouse Notch: a constitutively activated repressor of myogenesis directed at the basic helix-loop-helix region of MyoD. Development 120, 2385–2396.
Lai, E.C., 2004. Notch signaling: control of cell communication and cell fate. Development 131, 965–973.
Langdon, T., Hayward, P., Brennan, K., Wirtz-Peitz, F., Sanders, P., Zecchini, V., Friday, A., Balayo, T., Martinez, A.A., 2006. Notch receptor encodes two structurally separable functions in Drosophila: a genetic analysis. Dev. Dyn. 235, 998–1013.
Latimer, A.J., Appel, B., 2006. Notch signaling regulates midline cell specification and proliferation in zebrafish. Dev. Biol. 298, 392–402.
Le Gall, M., De Mattei, C., Giniger, E., 2008. Molecular separation of two signaling pathways for the receptor. Notch. Dev. Biol. 313, 556–567.
López, S.L., Paganelli, A.R., Siri, M.V., Ocaña, O.H., Franco, P.G., Carrasco, A.E., 2003. Notch activates sonic hedgehog and both are involved in the specification of dorsal midline cell-fates in Xenopus. Development 130, 2225–2238.
López, S.L., Rosato-Siri, M.V., Franco, P.G., Paganelli, A.R., Carrasco, A.E., 2005. The Notch-target gene hairy2a impedes the involution of notochordal cells by promoting floor plate fates in Xenopus embryos. Development 132, 1035–1046.
Lowell, S., Benchoua, A., Heavey, B., Smith, A.G., 2006. Notch promotes neural lineage entry by pluripotent embryonic stem cells. PLoS. Biol. e121, 4.
Ma, Q., Kintner, C., Anderson, D.J., 1996. Identification of neurogenin, a vertebrate neuronal determination gene. Cell 87, 43–52.
Mir, A., Kofron, M., Heasman, J., Mogle, M., Lang, S., Birsoy, B., Wylie, C., 2008. Long- and short-range signals control the dynamic expression of an animal hemisphere-specific gene in Xenopus. Dev. Biol. 315, 161–172.
Mizutani, K., Yoon, K., Dang, L., Tokunaga, A., Gaiano, N., 2007. Differential Notch signalling distinguishes neural stem cells from intermediate progenitors. Nature 449, 351–355.
Nieuwkoop, P., Faber, J., 1994. Normal Table of *Xenopus laevis* (Daudin). Garland Publishing, Inc., New York and London.
Oda, H., Akiyama-Oda, Y., 2008. Differing strategies for forming the arthropod body plan: lessons from Dpp, Sog and Delta in the fly Drosophila and spider Achaearanea. Dev. Growth Differ. 50, 203–214.
Oda, H., Nishimura, O., Hirao, Y., Tarui, H., Agata, K., Akiyama-Oda, Y., 2007. Progressive activation of Delta-Notch signaling from around the blastopore is required to set up a functional caudal lobe in the spider Achaearanea tepidariorum. Development 134, 2195–2205.
Pizard, A., Haramis, A., Carrasco, A.E., Franco, P., López, S., Paganelli, A., 2004. Whole-mount in situ hybridization and detection of RNAs in vertebrate embryos and isolated organs. Curr. Protoc. Mol. Biol. Chapter 14, Unit 9.
Przemeck, G.K., Heinzmann, U., Beckers, J., Hrabe de Angelis, M., 2003. Node and midline defects are associated with left–right development in Delta1 mutant embryos. Development 130, 3–13.
Rao, Y., 1994. Conversion of a mesodermalizing molecule, the Xenopus Brachyury gene, into a neuralizing factor. Genes Dev. 8, 939–947.
Schroeder, T., Meier-Stiegen, F., Schwanbeck, R., Eilken, H., Nishikawa, S., Hasler, R., Schreiber, S., Bornkamm, G.W., Nishikawa, S., Just, U., 2006. Activated Notch1 alters differentiation of embryonic stem cells into mesodermal cell lineages at multiple stages of development. Mech. Dev. 123, 570–579.
Sherwood, D.R., McClay, D.R., 1999. LvNotch signaling mediates secondary mesenchyme specification in the sea urchin embryo. Development 126, 1703–1713.
Sherwood, D.R., McClay, D.R., 2001. LvNotch signaling plays a dual role in regulating the position of the ectoderm–endoderm boundary in the sea urchin embryo. Development 128, 2221–2232.
Shivdasani, R.A., 2002. Molecular regulation of vertebrate early endoderm development. Dev. Biol. 249, 191–203.
Shook, D., Keller, R., 2003. Mechanisms, mechanics and function of epithelial–mesenchymal transitions in early development. Mech. Dev. 120, 1351–1383.
Stern, C.D., 2005. Neural induction: old problem, new findings, yet more questions. Development 132, 2007–2021.
Taira, M., Otani, H., Saint-Jeannet, J.P., Dawid, I.B., 1994. Role of the LIM class homeodomain protein Xlim-1 in neural and muscle induction by the Spemann organizer in Xenopus. Nature 372, 677–679.
Ueno, S., Kono, R., Iwao, Y., 2006. PTEN is required for the normal progression of gastrulation by repressing cell proliferation after MBT in Xenopus embryos. Dev. Biol. 297, 274–283.
Wardle, F.C., Smith, J.C., 2004. Refinement of gene expression patterns in the early Xenopus embryo. Development 131, 4687–4696.
Weber, H., Symes, C.E., Walmsley, M.E., Rodaway, A.R., Patient, R.K., 2000. A role for GATA5 in Xenopus endoderm specification. Development 127, 4345–4360.
Wettstein, D.A., Turner, D.L., Kintner, C., 1997. The Xenopus homolog of Drosophila suppressor of hairless mediates Notch signaling during primary neurogenesis. Development 124, 693–702.
Wittenberger, T., Steinbach, O.C., Authaler, A., Kopan, R., Rupp, R.A., 1999. MyoD stimulates delta-1 transcription and triggers notch signaling in the Xenopus gastrula. EMBO J. 18, 1915–1922.
Yasuo, H., Lemaire, P., 2001. Generation of the germ layers along the animal–vegetal axis in Xenopus laevis. Int. J. Dev. Biol. 45, 229–235.
Zhang, C., Klymkowsky, M.W., 2007. The Sox axis, Nodal signaling, and germ layer specification. Differentiation 75, 536–545.
Zhang, C., Basta, T., Hernandez-Lagunas, L., Simpson, P., Stemple, D.L., Artinger, K.B., Klymkowsky, M.W., 2004. Repression of nodal expression by maternal B1-type SOXs regulates germ layer formation in Xenopus and zebrafish. Dev. Biol. 273, 23–37.